Integrating the metabolic processes of *Escherichia coli* with virulence by decreasing glucose availability, inhibiting the acetyl-CoA carboxylase gene *accA* with asRNA, and through the quantification of the *luxs* gene

Tatiana Hillman1

1 Biological Sciences, TheLAB, Inc., Los Angeles, California, United States

Corresponding author:

Tatianna Hillman1

Email address: thillman@usc.edu

ABSTRACT

The study aims to demonstrate a possible link between bacterial cell metabolism and virulence by combining the metabolic mechanisms of the gram-negative bacteria, *Escherichia coli*. Glucose increases the proliferation of intestinal microflora. The bacterial microflora ferment glucose into short-chain fatty acids and long-chain fatty acids. Bacteria synthesize long-chain fatty acids for plasma membrane and biofilm formation. *Escherichia coli* was cultured in Luria broth, enhanced with a high to a low concentration of glucose to increase the synthesis of acetyl-CoA carboxylase. The 15mM sample yielded 4,210ng/µL of qPCR products measured for the target gene *accA*. The 7.5mM sample produced a concentration equal to 375 ng/µL, and the control sample measured an *accA* concentration of 196 ng/µL. The gene *accA*, one of four subunits for the acetyl-CoA carboxylase enzyme, was suppressed by asRNA, producing a qPCR product of 63 gene copies. Antisense RNA for *accA* reduced the amount of *luxs*, a vital gene needed for propagating quorum-sensing signal molecules. The *luxs* gene, which is responsible for releasing autoinducer-2 for intercellular quorum sensing, was reduced by the gene inhibition of *accA* with asRNA. The increase in *luxs* transcription augments biofilm production in support of spreading virulence. An antibiotic resistance test was performed that implanted disk containing tetracycline, carbenicillin, and chloramphenicol unto cultures expressing antisense RNA. Bacterial cells that were transformed with the antisense inducible vector, for inhibiting *accA,* displayed more antibiotic susceptibility. The implications of the study advocate for designing antibiotics that target bacterial cell metabolic processes to block bacterial antibiotic resistance.

INTRODUCTION

Alexander Fleming discovered penicillin in 1928. His discovery began the use of antibiotics that saved many lives; however, with the overuse of antibiotics, the issue of antibiotic resistance has occurred in parallel. Between the 1960s and the 1980s, a profound formulation of many new and novel antibiotics were discovered [1]. The new and novel antibiotics could not supersede the vigorous evolution of bacterial antibiotic resistance. The three phases that occur after bacterial horizontal gene transfer for proliferating antibiotic resistance include: 1) the antibiotic genes received during conjugation code for the creation of efflux pumps; 2) the antibiotic-resistant genes enclosed inside the pre-antibiotic genes impede the antibiotic drugs attaching to the antibiotic gene target sites; 3) the antibiotic-resistant genes direct the ubiquitous destruction of antibiotic drugs through hydrolysis [2].

Fleming's discovery came after he observed a growth of mold that reduced the population of staphylococci cultured in a petri-dish [3]. He published his findings for the first antibiotic discovered called penicillin. More researchers, in 1940 began to publish a description for the methods of isolating large quantities of penicillin for clinical studies [4]. Due to the studies of penicillin conducted by the researchers from Oxford University, penicillin became a well-known and highly administered antibiotic in the year of 1945. Since penicillin first use in 1945, antibiotic resistance has amplified [5].

Bacteria can adapt to any and to multiple environments. Adding antibiotics to the environment of a bacterium pressures it to create gene mutations called antibiotic resistant genes. The bacterium also shares those antibiotic resistant genes with other bacteria. The process of natural selection is immensely active and central for the development of antibiotic resistance. For example, persister cells are the bacterial cells that survived its contact with antibiotics. The persister cells survive to initiate and spread antibiotic resistance after its exposure to antibiotics [6]. The bacteria of *A. baumanii* inhabit hospitals, is highly contagious, and develops antibiotic resistance through horizontal gene transfer. The *A. baumanii* bacterium cause 64% of urinary tract infections during the use of catheters [7].

Only a few of the novel antibiotics were available to treat many of the antibiotic-resistant bacterial infections. Therefore, there has been a reduction in the field of pharmaceutics to design more new and novel antibiotics. Therefore, more future research should investigate the processes, mechanisms, and dynamics of antibiotic resistance to increase the development of potent antibiotics. Antimicrobial resistance or AMR has led to the deaths of 700,000 annually, including an additional 10 million people who are approximated to die by 2050 [1]. However, generating novel antibiotics has not solved the problem of AMR since bacterial resistance has reduced the efficacy of every antibiotic administered in the clinical setting. There is a demand for more creative and advanced antibiotics to deal with this massive public health issue. The microbial formation of biofilm contributes to that spread of antibiotic resistant genes and bacteria.

The bacterial colonies within biofilms are profusely resistant to antibiotics, and the biofilm induces the continuance of chronic infections. Because the extracellular biofilm matrix prevents penetration of antibiotics, is mostly anaerobic, or lacking oxygen, bacteria within the biofilm are more tolerant of antibiotics [8]. Biofilms are an organization of bacterial groups

attached to a biotic or abiotic extracellular matrix. However, there is insufficient knowledge about the effect of antibiotic-resistant processes linked to bacterial biofilms. Bacteria use the formation of biofilm as a profitable survival strategy.

Biofilm allows bacterial cells to develop a high tolerance for antibiotics through resistance. The biofilm formed consists of proteins, extracellular DNA, sugars, and is strongly resistant to proration by antibiotics. The antibiotics administered can eradicate most of the bacteria cells on the surface of the biofilm, but the bacteria embedded closer to the base of the matrix remain [9]. Biofilm can endure and persist after antibiotic exposure due to many physical, anatomical, and innate genetic factors. The pathogenic bacteria create many of the virulent actions that increase biofilm production through quorum sensing or cell to cell communication. Due to the cell-cell communication for biofilm formation, designing small molecules for disturbing the quorum-sensing signals can inhibit biofilm development.

After researchers exposed bacterial cells within biofilm to the antibiotics to rifampicin- and kanamycin-resistant mutants within immature biofilm communities, the results displayed that each mutant amplified in growth without the presence of antibiotics. Researchers treated the mutant cultures with kanamycin and found that the biofilm showed a reduction in antibiotic resistance. However, after 250 generations, the resistant mutant bacteria increased in growth at the surface and the base of the biofilm matrix [10]. *Pseudomonas aeruginosa* can produce reactive redox pigments. These pigments are called phenazines, which affect the expression of genes, cause metabolic changes, and can alter the tolerance of the bacterial cells of antibiotics [11]. Phenazines induce the survival of *P. aeruginosa* through its ability to modify biofilm physiology. Phenazines increase the formation of the initial matrix, composed of exopolysaccharide, which is needed for bacteria to attach and form a mature biofilm. The Phenazines cause the production of efflux pumps and affect the downward cascade of the central metabolic processes of *P. aeruginosa*. Researchers measured the bacterial mutant-survivors of biofilm after exposure to antibiotics and a carbon compound. They found that after biofilms of *P. aeruginosa* were cultured with succinate, a carbon component that enters the mid-central metabolism of glucose, the phenazine could no longer protect bacterial cells from antibiotic penetration and eradication.

Therefore, a bacteria's increased tendency to develop bacterial populations of biofilm is a significant factor of virulence. For example, most patients suffering from a skin infection known as *S. epidermidis* produce an active biofilm in vitro [12]. The exopolysaccharide matrix can lessen the penetration of the deeper strata of the biofilm by antibiotics. Exposing bacteria to antibiotics at the deeper layers of the biofilm forms resistant mutants of those bacteria [13]. After administering more massive amounts of antibiotics for more extended periods, the biofilm communities of bacteria can remain active, live, and survive.

Lux-S is necessary for the motility of bacteria and for forming a bacterial biofilm. Lux-S is an S-ribosylhomocysteine lyase that produces autoinducer-2. Autoinducer-2 is a signaling molecule released that induces the cell to cell communication called quorum sensing. Bacterial cells communicate through an intercellular process called quorum sensing. Amplified Lux-S expression increases the release of autoinducer-2, intensifies quorum sensing, and produces more biofilm for spreading pathogenic bacteria. The expression of the gene *luxs* induces the release of autoinducer-2. Quorum sensing is a type of communication between bacterial cells that occurs

121 through the release of small signaling molecules called autoinducers. Releasing the autoinducers
122 regulates the aggregation of cells and monitors genetic expression. The autoinducers of gram-
123 negative bacteria consist of homoserine lactones versus gram-positive bacteria that release
124 oligopeptides [14]. The luxs gene is essential for synthesizing and releasing autoinducer-2.
125 However, the metabolism of glucose by bacteria significantly affects the output of autoinducers
126 and the production of biofilm. The acetyl-CoA carboxylase enzyme catalyzes the biosynthesis of
127 long-chain fatty acids and hydrolyzes glucose into short-chain fatty acids. The acetyl-CoA
128 transferase synthesizes LCFAs through the alpha subunit of ACCase, or the ACCA subunit
129 transfers a carboxyl group from pyruvate to an acetyl-CoA, producing malonyl-CoA.

130 Lux-S produces signals for quorum sensing, increases biofilm formation, and spreads
131 virulence. Inhibiting the fatty-acid synthesis of bacterial cell metabolism can reduce Lux-S
132 expression and biofilm production. Increased metabolic fatty-acid synthesis can amplify Lux-S
133 expression as a virulent producer of biofilm, which can cause the persistence of antibiotic-
134 resistant bacteria. We do not entirely understand the exact mechanism that connects cell
135 metabolism with the bacterial pathogenesis of antibiotic resistance. The author suggests that
136 blocking the enzymatic activity of acetyl-CoA carboxylase may represent a potential aim for
137 overcoming antibiotic resistance.

138 The metabolic processes of bacteria may provide much potential for generating and
139 designing novel therapeutics as antibiotics that can reduce biofilm formation. For example,
140 CbrAB is a membrane-bound histidine kinase, and a part of the metabolic regulatory system
141 called the CbrAB/Crc system [15]. The CbrAB/Crc system shows a connection between bacterial
142 cell metabolic processes with antibiotic resistance [16]. A process called catabolite repression
143 control or Crc inhibits the translation of catabolite activities by targeting specific mRNAs. The
144 Crc protein targets mRNAs that are adjacent to ribosome binding sites [17]. Limited sources of
145 carbon compounds cause the activation of the CbrAB/Crc system. The CbrAB protein initiates
146 the expression of a small RNA termed *crcz*. The crcz alleviates the repression of the Crc-targeted
147 mRNAs. Inhibiting the *crc* gene lowers the growth rate of bacteria along with providing a higher
148 susceptibility to antibiotics [16].

149 Nutrient availability can determine the expression of metabolic genes and remove the
150 bacterial response of antibiotic resistance. In a study by Peng et al. (2015), bacteria cultured
151 without glucose or the non-polar amino acid of alanine were less susceptible to kanamycin, an
152 antibiotic. Only 9.5 ng/mL of the kanamycin was absorbed; however, adding alanine and glucose
153 to the cultures increased the uptake of kanamycin to 65-123 ng/mL and then to 113-231 ng/mL
154 [18]. Shu et al. (2018) performed a Michaelis-Menten kinetics experiment using multi-drug
155 efflux pumps while adding glutamate and acetate to growths of *Escherichia coli* [18]. They
156 confirmed that the *Escherichia coli* cells were more sensitive to gentamicin, which is an
157 antibiotic. Each of the previously mentioned studies displays a significant link between bacterial
158 metabolism and antibiotic resistance.

159 For that reason, we tested the effects of extracellular nutrient availability on bacterial
160 gene expression. We altered the concentration of glucose in Luria-Bertani broth media. RNA
161 was extracted to test the yield of the gene expression of *Escherichia coli*. To study the
162 intracellular process, the gene expression of *accA,* a subunit of the acetyl-CoA carboxylase
163 enzyme, was quantified via real-time PCR. The ACCase complex is an essential enzyme for the

first step of the bacterial fatty acid synthesis. The cell metabolism within *Escherichia coli* cells induces the expression of the four genes, *accA, accB*, *accC*, and *accD*, which code for the translation of acetyl-CoA carboxylase. The four genes for acetyl-CoA carboxylase modify the composition of fatty acids and monitor the rate of production. The four genes also monitor the overexpression of ACCase by inserting one of the four subunits, activating antisense RNA expression [19]. When quantifying the activity of ACCase, the concentration of the gene *accA* was measured. We conjoined the exposure to glucose with antisense RNA inhibition.

We suppressed the *accA gene*, using antisense RNA transcripts, to measure the effects of genetic inhibition of the intracellular metabolic processes and recorded the subsequent RNA concentrations. The original bacterial protocell constrains foreign and movable DNA through the transcription of antisense RNA, which is complementary to its specific DNA target sequence [20]. The asRNAs bind to the sequences flanking the ribosome-binding site and the start codon of the target mRNAs [21]. The antisense RNA blocks the ribosomal detection by the RBS inhibiting translation [21]. In this study, antisense RNA obtained amplification through the PCR amplification of an antisense DNA sequence. The DNA flanked at the XhoI, and NcoI restriction sites converted the sequences into antisense RNAs. We implanted the PCR product into the pHN1257 plasmid through ligation (Fig 1). Also, *Escherichia coli* cells were induced into antisense expressing bacteria after transforming the competent bacteria cells with the recombinant IPTG-PT-asRNA plasmid called pHN1257. Real-Time PCR analysis was performed to determine the number of gene copies for *accA.*

Figure 1 Plasmid Assembly and the Gene Silencing of *accA*

Plasmid Assembly and Gene Silencing the PCR products and the PTasRNA expression vector of the plasmid pHN1257 were digested with the restriction enzymes XhoI (upstream) and NcoI (downstream). After the restriction digestion, the antisense PCR product was ligated into the IPTG-PTasRNA inducible vector of pHN1257 at the multiple cloning site.

doi: 10.3390/ijms15022773 This article is an open-access article distributed under the terms and conditions of the Creative Commons Attribution license (http://creativecommons.org/licenses/by/3.0/).
https://www.ncbi.nlm.nih.gov/pmc/articles/PMC3958881/figure/f6-ijms-15-02773/

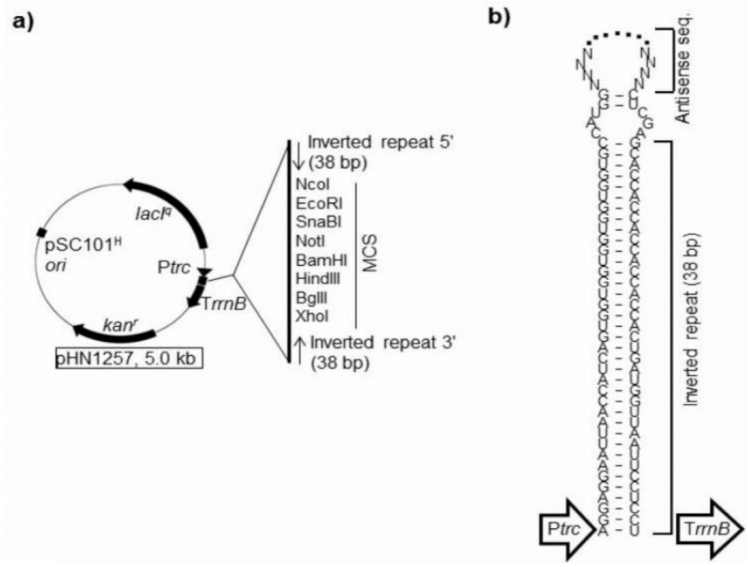

Also, suppressing the *accA* gene can model the mechanism of the pathogenic bacterial repression of gene transcription based on the availability of nutrients and any other physiological change [22]. We measured the effects of extracellular and intracellular factors upon the intercellular communication between cells by quantifying the gene copy number of *luxs*. We altered the concentration of glucose and inhibited the *accA* to analyze the correlation between glucose (extracellular), *accA* (intracellular), and *luxs (intercellular)* (Table. 1). An antibiotic resistance test was performed that implanted disk containing tetracycline, carbenicillin, and chloramphenicol unto bacterial cultures expressing antisense RNA. The author hypothesizes that inhibiting *accA* while lessening glucose availability will decrease the *luxs* gene copy number as quantified through qPCR. The author expects to determine an integration between extracellular glucose, intracellular metabolic gene expression, the effect of the two preceding stages of metabolism on intercellular cell-to-cell signaling, and pathogenesis. We further hypothesize that inhibiting metabolic genes as *accA* can help to reduce antibiotic resistance. The purpose of the study is to demonstrate the immense potential of targeting the metabolic gene, *accA,* for overcoming antibiotic resistance.

MATERIALS AND METHODS

BACTERIAL CELL CULTURE AND RNA EXTRACTION

The *Escherichia coli* TOP10 strain of cells were cultured and plated onto 25 mL agar plates. The bacterial cells were inoculated into Luria-Bertani broth, enhanced with glucose concentrations of 200µM, 50µM, and 0µM. The cultures of 200, 50, and 0 micromolar (n=7) of glucose were measured for the dsDNA and the RNA OD260 concentrations and replicated seven times. Varied concentrations of glucose, including, 15mM, 7.5mM, 5mM, and control of glucose were added to LB liquid with *Escherichia coli* cells. The plasmid pHN1257 was utilized for assembly of the antisense expression vectors. The recombinant plasmid of pHN1257 for the expression of antisense RNA was plated with the kanamycin antibiotic and incubated at 37°C for 24 hrs. Cells grown on agar plates were inoculated into 4 mL of LB liquid media with (+) and (-) PTasRNA bacterial cells expression of asRNA for *accA* cultured with kanamycin. A sum of 20 RNA extractions were completed. A total of 3 mL of bacterial cell culture from the cells grown in the varying concentrations of glucose, the (+) asRNA, and the (-) asRNA cells were centrifuged at 4,000 x g for 10 minutes at 4°C. The medium was discarded, and the cells were resuspended in 100µL of lysozyme/TE buffer. The solution was vortexed for 30 seconds. Incubation occurred at 30°C for 10 minutes in a shaker-incubator. A lysis buffer of 350µL with 25mg of glass beads was added. The lysates were centrifuged for 5 minutes at maximum speed. RNA was extracted using HiBind RNA mini columns through RNA Wash Buffers I and II. The RNA was eluted with 50µL of DEPC water.

CDNA PREPARATION

The author used the OneScript Reverse Transcriptase cDNA Synthesis kit by Applied Biological Materials Inc. or ABM. Approximately, 1µg of RNA from each sample, high glucose, medium glucose, low glucose, and (-) glucose were added to 0.5µM oligonucleotides(dT) (10µM). For the asRNA and (-) RNA, one microgram of each total RNA extract was added to the initial primer/RNA and reaction mixture. The cDNA was also prepared for *luxs* quantification. The original primer/RNA mix consisted of 1µg of total RNA, 1µL of oligo(dt), 1µL of dNTP (10mM) mix, and nuclease-free water for a 20µL reaction solution. The mixture was heated to 65°C for 5 minutes and then incubated on ice for 1 minute. The reaction mixture of 4µL 5X RT buffer, 0.5µL of RNaseOFF, and 1µL OneScript RTase was added to the original primer/RNA mix in a 2µL microcentrifuge tube. The cDNA was synthesized by incubating the tube for 50 minutes at 42°C. The reaction was stopped at 85°C for 5 minutes and chilled on ice. The cDNA was stored at -20°C.

PCR

A Promega PCR MasterMix volume of 25µL was added to the upstream and downstream primers, each of 0.5µL specific for the *accA* gene target. PCR amplification was repeated as a triplicate. The concentrations of the two cDNA samples added to the PCR master mix were 190ng and 230ng plus nuclease-free water. A 2X and 1X upstream primer, 10µM 0.5–5.0µl0.1–1.0µM, and a downstream primer, 10µM 0.5–5.0µl 0.1–1.0µM, DNA template 1–5µl less than 250ng, and nuclease-free water were mixed into a 50µl PCR reaction mixture. The thermocycler was set to denaturation of a 2-minute initial denaturation step at 95°C. Other subsequent

272 denaturation steps were between 30 seconds and 1 minute. The annealing step was optimized
273 with annealing conditions by performing the reaction starting approximately 5°C below the
274 calculated melting temperature of the primers and increasing the temperature in increments of
275 1°C to the annealing temperature. The annealing step was set at 30 seconds to 1 minute at 52°C.
276 For the extension reaction with Taq polymerase, there was 1 minute allowed for DNA to be
277 amplified at 72°C with a final extension of 5 minutes at 72–74°C. The PCR thermocycler
278 completed 40 cycles of amplification instead of 35 cycles.

279 **AGAROSE GEL ELECTROPHORESIS AND PLASMID ASSEMBLY**

280 The condition of the PCR products, without primer dimers and contamination, for the
281 target gene *accA,* were detected through agarose gel electrophoresis. The PCR products were
282 confirmed without primer dimers and contamination, the PCR products, and the PTasRNA
283 expression vector of the plasmid pHN1257 were digested with the restriction enzymes XhoI
284 (upstream) and NcoI (downstream) (New England Biolabs XhoI- catalog R0146S- 1,000 units
285 and NcoI- catalog R0193S- 1,000 units) (Fig. 1). Each microcentrifuge tube was placed in the
286 incubator for 30 minutes at 37°C. A heat block was heated to 90°C. The PCR products of the
287 *accA* gene were ligated into the pHN1257 plasmid by mixing 1µL of the DNA insert with 2µL of
288 the plasmids, adding 5µL of ligation mix, and then placing the tubes into a heat block of 90°C
289 for 15 minutes (Takara Ligation Kit 6023). Competent bacterial cells were transformed with the
290 pHN1257plasmid plus the antisense DNA insert of *accA,* for expressing (+) asRNA and (-)
291 asRNA, which is the control. The competent cells were incubated with the recombinant DNA for
292 45 minutes at 37oC.

293 **REAL-TIME PCR**

294 The author enhanced each bacterial sample with the glucose concentrations of 15mM,
295 7.5mM, 5mM, and 0mM (n=3). A triplicate of real-time PCR experiments was completed. The
296 cDNA from H-glucose, M-Glucose, L-glucose, and the control (-) glucose were diluted into a 1:8
297 serial dilution. A 10-fold dilution of standards was prepared for bacterial samples transformed
298 with (+) asRNA inducible plasmids and exposed to high to a low volume of glucose. The amount
299 of gene expression for *accA* and the target gene *luxs* were measured through absolute
300 quantification methods of qPCR. The diluted cDNA was pipetted into a transparent 96 well plate.
301 A 0.4µl of each primer pair mixture was pipetted into a microcentrifuge tube with 10µL of
302 SensiMix SYBR MasterMix, and with 1.2µL of DEPC water. The SYBR reaction mixture of
303 12µL was then pipetted into the wells with the diluted and undiluted cDNA. The optical film
304 sealed the plate. The PCR plates were centrifuged for 2 minutes at 2500 rpm to reposition all
305 liquids to the bottom of the wells. The real-time PCR Amplification Protocol (Roche Lightcycler
306 480 machine) began with a 3 min step at 95°C for 40 cycles with a step of 10 sec at 95°C, 45 sec
307 at 65°C, and 20 sec at 78°C with one step of 1 min at 95°C. One step of 1 min at 55°C for 10s
308 each started at 55°C with a 0.5°C increment at each step up to 95°C. For the Roche Lightcycler
309 480 machine, the 96-well clear Roche plates were used for SYBR green detection.

310

311

312 **THE qPCR ABSOLUTE QUANTIFICATION OF LUX-S**

313 Bacterial cells were transformed with the pHN1257 plasmid expressing asRNA to inhibit
314 the genetic expression of the *accA* gene. Three replications of qPCR were performed for
315 quantifying the gene copies of *luxs*. The author added 25µM and 5µM concentrations of glucose
316 to the bacterial samples expressing antisense RNA for the inhibition of the gene *accA.* RNA was
317 extracted from cells grown with 25µM glucose and 5µM of glucose. The cells grown with
318 glucose in the medium were also transformed with antisense expressing IPTG-PT-asRNA
319 inducible pHN1257plasmids. Cells were cultured without (-) glucose, but the expression of *accA*
320 was also inhibited, (+) asRNA. A control, without (-) glucose and (-) asRNA, was compared to
321 each sample. The number of gene copies for *luxs* was measured through the qPCR amplification
322 protocol and absolute quantification (Roche Lightcycler 480 machine).

323 **ANTIBIOTIC RESISTANCE TEST**

324 Competent T7 bacteria cells were transformed with the inducible vector termed pHN1257
325 that expressed antisense RNA to inhibit the gene *accA.* The newly transformed bacteria cells
326 were plated unto nutrient agar medium consisting of the antibiotic kanamycin. Three to five
327 colonies from the pHN-1257-asRNA-*accA* bacterial transformants were selected and cultured in
328 LB broth, enhanced with kanamycin, for 18 to 24 hours at 37 degrees Celsius in a shaking
329 incubator. A control group that did not express asRNA for *accA* was cultured in LB broth
330 overnight at 37 degrees Celsius. One hundred microliters of the pHN1257-asRNA-*accA* and
331 from the control group were pipetted unto nutrient agar petri dishes (N=64) containing 50
332 micromolar of the kanamycin antibiotic for the sample of pHN1257-asRNA-*accA* . A swab was
333 used to spread the 100 microliters of each experimental (with asRNA) and the control (without
334 asRNA) unto the agar plates to form a lawn of bacterial growth. The six-millimeter sized disks
335 contained 5 microliters of each the three consecutive antibiotics, including tetracycline,
336 carbenicillin, and chloramphenicol. Each group of eight disks were prepared with tetracycline,
337 carbenicillin, and chloramphenicol. The antibiotic disks were placed unto the agar plates that
338 were divided into 4 or 8 sections. The bacterial cultures grew for 18-24 hours at 37ºC. The zone
339 of inhibition for each of the disk (N=64) were measured in mm and compared to a chart for
340 Antibiotic Resistance and Susceptibility Tests.

341 **STATISTICAL ANALYSIS**

342 Figures were constructed with the Sigma Plot 14th edition, Microsoft excel, and the 8th
343 edition of GraphPad Prism. The mean and standard deviations were calculated by Microsoft
344 Excel and GraphPad Prism. The p-values and the ANOVA results were produced through
345 GraphPad Prism. Standard error bars for each figure were added through Sigma Plot. The
346 standard curves for the absolute quantification of the genes *accA* and *luxs* were generated
347 through Microsoft excel with linear regression coefficients added and calculated for each
348 standard curve for the absolute quantification of *accA* and *luxs*. The antibiotic resistance test was
349 analyzed, given descriptive statistics, and generated paired-t test results through the OriginPro
350 2019B software. A t-test and a density graph for antibiotic susceptibility of pHN1257(+) asRNA
351 for *accA* was produced through the OriginPro 2019B computer application. The p-value was
352 calculated from the t-score and the degrees of freedom for the antisense versus the control of the
353 bacterial growths' sensitivity to the antibiotics.

354 **TABLE 1 A Summary of the Bacterial Sample Treatments**

Bacterial Sample	Treatment	Concentration (mM/µM)
Gluc-200	glucose	200 µM
Gluc-50	glucose	50 µM
Gluc-0	glucose	0 µM
H-glu	glucose	15mM
L-Glu	glucose	5mM
M-Glu	glucose	7.5mM
Control-Glu	glucose	0mM
H-glu	glucose & (+) asRNA-*accA*	15mM
L-Glu	glucose & (+) asRNA-*accA*	5mM
M-Glu	glucose & (+) asRNA-*accA*	7.5 mM
Control-Glu	(+) asRNA-*accA*	0mM
(+) asRNA-*accA*	(+) asRNA	N/A
(-) asRNA-*accA*	(-) asRNA	N/A
25-glu- (+)asRNA-*accA*	glucose & (+) asRNA	25 µM
5-glu- (+)asRNA-*accA*	glucose and (+) asRNA	5 µM

(+) asRNA-*accA*	**(+) asRNA**	**N/A**
(-) asRNA-*accA*	**(-) asRNA**	**N/A**

355 **A Summary of the Bacterial Sample Treatments** Samples of *E. coli* were prepared with 200,
356 50, and 0 µM of glucose for dsDNA detection through an OD260 analysis. Bacterial colonies
357 were treated with 15, 5, 7.5, and 0 mM concentrations of glucose for RNA and qPCR product
358 quantification of the gene *accA*. The 25 µM and 5 µM of glucose bacterial samples were treated
359 with antisense RNA for *accA* inhibition and the qPCR products for *luxs* were measured. *E. coli*
360 colonies were provided with antisense RNA for *accA*, (+)asRNA, and cultured without antisense
361 RNA, (-)asRNA, for quantifying the number of gene copies for *luxs*.

362 **RESULTS AND DISCUSSION**

363 **THE EFFECT OF GLUCOSE ON THE RNA CONCENTRATION AND THE**
364 **EXPRESSION OF ACCA**

365 Hydrolytic enzymes of *Escherichia coli* split one glucose molecule into two pyruvates.
366 The acetyl-CoA carboxylase enzyme transfers a carboxyl group from the pyruvate to the acetyl-
367 CoA, producing malonyl-CoA (Fig 2). The acetyl-CoA carboxylase enzyme consists of four
368 subunits combined into the AccABCD complex. The *accA* gene codes for the ACCA subunit,
369 which is the transferase domain of the ACCase enzyme. From the results, the genetic expression
370 of *accA* was proportional to the increased glucose concentrations in *Escherichia coli* bacterial
371 samples. After culturing *Escherichia coli* with different levels of glucose, the RNA
372 concentrations for each sample measured were of 1392, 797, 608, and 199 ng/µL for the H-
373 Glucose, M-Glucose, the L-Glucose, and the control, respectively. The genes of *accA* and *accD*
374 are entirely independent of the *accBC* operon.

375 The overexpression of *accB* blocks the transcription of *accBC*; however, the
376 overexpression of *accA and accD* does not affect the activity of the *accBC* operon [23]. A high
377 level of glucose increases the availability of *accB*, and the transcription of the *accBC* operon is
378 significantly reduced even after exposure to a small amount of *accB*. Although a high glucose
379 concentration can stymie the production of *accBC*, the over-activated *accBC* operon did not
380 inhibit the production of *accA,* the target gene of study. The subunit ACCA encoded in the *accA*
381 gene may act as a more intense target for blocking bacterial cell fatty acid synthesis and
382 metabolism. The *Escherichia coli* TOP10 bacteria cells were grown in LB broth overnight at
383 37°C with 15mM (High-glucose), 7.5mM (Medium-glucose), 5mM (Low-glucose), and control
384 of glucose concentration (Fig 3). RNA was extracted from each sample and the concentrations
385 determined by the Implen Nanophotometer 250. The high-glucose sample produced the highest
386 amount of RNA compared to the medium, the low, and to the control. The RNA for each sample
387 was reverse transcribed into the first-strand cDNA, and absolute quantification with qPCR
388 measured the amount of the target gene, *accA,* of each sample.

389

Figure 2 Formation of Malonyl-CoA The hydrolysis of glucose molecules into two pyruvates yields the ACCase enzyme. The acetyl-CoA carboxyl transferase or the ACCA alpha subunit of the acetyl-CoA carboxylase complex, AccABCD, transfers a carboxyl group from the pyruvate to the acetyl-CoA to form malonyl-CoA. The malonyl-CoA enters the fatty acid synthesis pathway, elongating fatty acids into long-chain fatty acids of phospholipids necessary for structuring plasma membranes and for forming the initial extracellular matrix.

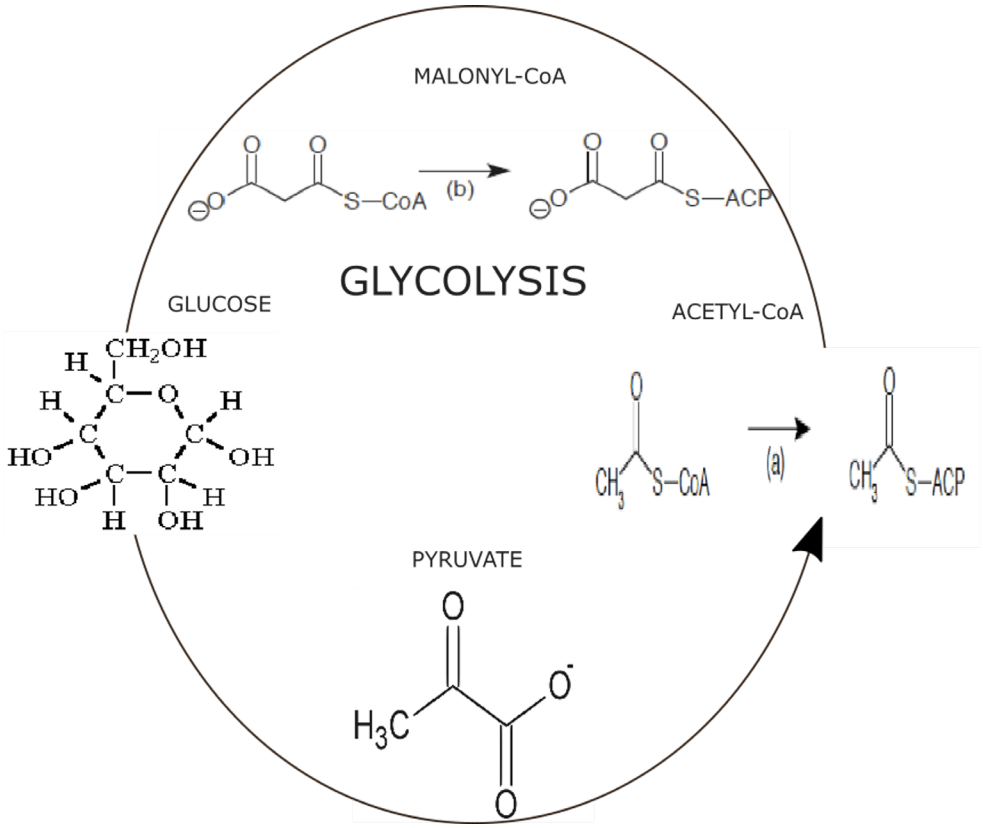

A) **Figure 3 Glucose concentration versus RNA** Glucose concentrations of 15mM, 7.5mM, 5mM, and the control samples each yielded RNA concentrations, in ng/µL, 1392, 797, 608, 179, respectively. A) The bacterial sample with 15mM glucose yielded the most substantial measure of RNA, noting a proportional relation between glucose and genetic expression of *E. coli*. B) The results display the qPCR results for 15mM, 7.5mM, 5mM, and the control. The samples with 15mM and 5mM glucose displayed the most genetic activity of *accA* transcription, measuring *accA* concentrations of 4,210 ng/µL and 1,500 ng/µL, respectively. The *accA* qPCR concentrations for 7.5mM *accA* equaled 372 ng/µL and a 196 ng/µL quantity for the control. C) The analysis displays the OD260 measure of DNA results for samples of *E. coli* grown in medium enhanced with 200µM, 50µM, 0µM of glucose.

410

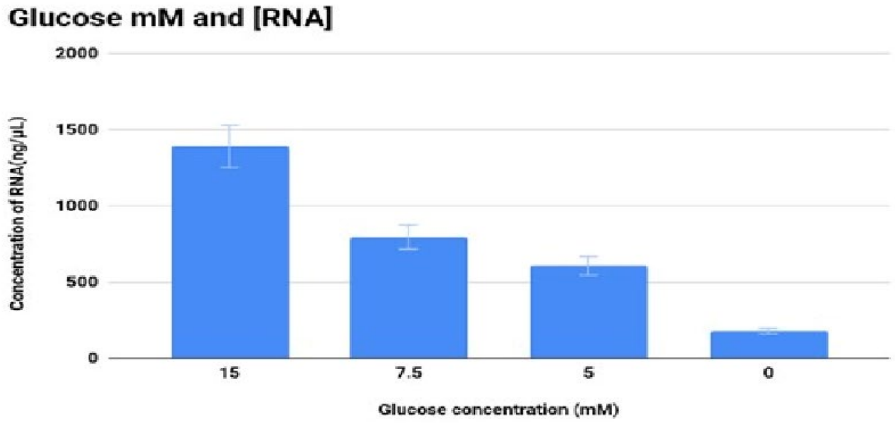

A)

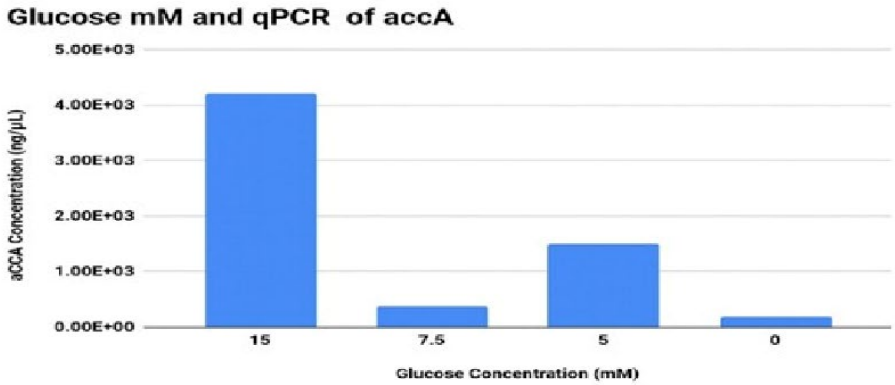

B)

411

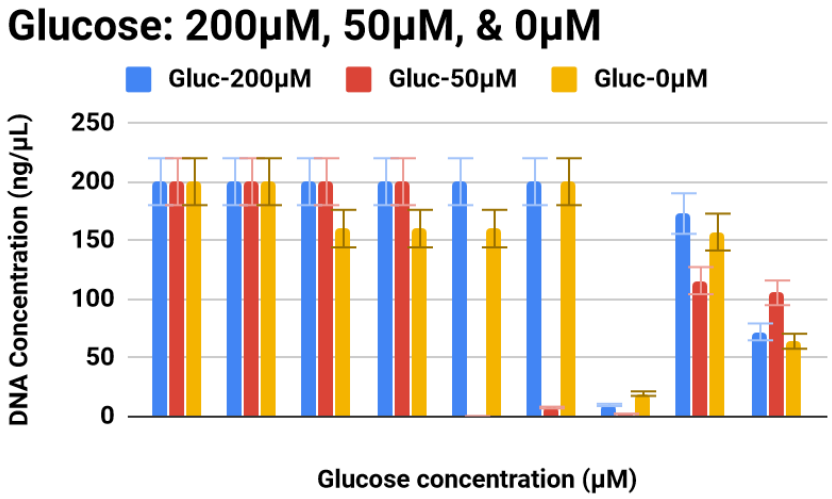

412

413 C)

The RNA of each bacterial sample enhanced with glucose was extracted and the concentrations determined (N=20, 335.4 ± 329.2). The high-glucose sample provided a crossing point value or a Cp-value of 12.28, and the concentration of *accA* was 4.21E3 ng/µL. The Cp of the sample of medium-glucose equaled 16.51 with a concentration of 3.75E2, and the low-glucose Cp was 14.08 with a target gene concentration of 1.50E3 (Fig 3). The concentration of *accA* by qPCR analysis, in ng/µL, included: 4210, 375, 1500, and 196 for H-glucose, M-glucose, L-glucose, and for the control, respectively. The number of qPCR products ranged from 11-186, 5-18, and 0-79 gene copies for High-glucose, Medium-glucose, and the Low-glucose/control, respectively (N=12, 48±38).

The control group produced a Cp value of 17.64 with a target gene concentration of 1.96E2. For the glucose concentrations of 200µM (n=7,173±72), 50 µM (n=7,116±105), and the control (n=7, 157±64) compared to their dsDNA concentrations showed significant variability (Fig 3). Comparing 200 µM to its control group, the difference between the samples was statistically significant (p=0.038). The cells grown in 200µM yielded a more significant and more abundant production of dsDNA than cells cultured as a control. After loading a 96-well plate for qPCR with 8-fold dilution standards of each sample, the standards of each sample were used to calculate a standard curve (Fig 3).

Vinals et al., (1999), found that a high glucose concentration blocks the absorption of glucose as a result of its repression of glucose phosphorylation [24]. Ferraris et al. (1990), measured the luminal glucose osmolarity and the concentrations in the small intestines. They found that the luminal glucose concentrations in a range of 50mM to 500mM exhibited errors [25]. The previous researchers measured glucose concentrations but did not recognize how osmolality is affected by Na+ and K+ salts, amino acids, and peptides [25]. Ferrais et al. (1990), discovered that the average of SI luminal osmolarities was approximately 100 mosmol/kg, which were mainly hypertonic results. In the Ferrais et al. (1990) study, for an animal's diet, the SI glucose concentrations averaged 0.4-24 mM and ranged with time over a large amount of an SI region from 0.2 to 48 mM. There was a 60 percent reduction of 2-deoxyglucose uptake at 30 mM glucose from their study [25]. The high glucose osmolality resulted in a reduced Vmax value for 2-deoxyglucose uptake with a constant Km, calculated from the Michaelis-Menten kinetic enzyme equation [25]. It was also found that high concentrations of glucose lessened the absorption of glucose in endothelial cells called ECV304 cell lines [24].

THE QPCR RESULTS OF THE ANTISENSE RNA INHIBITION OF THE TARGET GENE ACCA

Ninety percent of the genome for Eukaryotes consists of non-coding regions or RNA that will not translate into proteins. Antisense transcription is the purpose of the noncoding regions of human cell DNA [26]. The non-coding transcripts are called natural antisense RNAs. Researchers have recorded antisense activity in mice, *Saccharomyces cerevisiae*, *Drosophila melanogaster*, and *Arabidopsis thaliana* [27]. The production of recombinant DNA required the ligation of the PCR product of the gene insert, *accA,* into the plasmid pHN1257 (Fig. 1). The re-engineered pHN1257 amplified the expression of antisense RNA. The PCR product and the IPTG-PT-asRNAs plasmid of pHN1257 were cut with the restriction enzymes XhoI and NcoI. The primers (Table. 2) each contained an extra 3 to 4 bps of nucleic acids to accompany the sequences for Xhol and NcoI. The primers flanked the target DNA, which totaled to 150 base

457 pairs. The antisense sequence was constructed in a specific orientation in that the restriction sites,
458 which NcoI normally flanks the forward primer, reversed positions. The XhoI was repositioned
459 to flank the forward primer, and the Nco1 flanked the reverse primer, creating the antisense
460 sequence when inserted into the plasmid for pHN1257. The PCR product was amplified (n=3,
461 219 ± 171), and then ligated into the pHN1257-asRNA inducible vector.

462 **Table 2 Primers for amplifying the *luxs* gene, antisense RNA for *accA,* and the *accA* gene.**
463

Primers	DNA Sequence
XhoI+*accA* Forward	GAGATGAGTCTGAATTTCCTTGATT
NcoI+*accA* Reverse	TGGCAGTTCATCGCTTTTTTCAC
luxs Forward	CATACCCTGGAACATCTGTTTGC
luxs Reverse	AGTTCCTGCACTTTCAGCACATC
accA Forward	TCATCACCTTTATCGACACCCC
accA Reverse	TTCACTTTATCGCCCACGCC

464

465 **The Primers for PCR Amplification and qPCR Analysis** To produce antisense RNA for *accA*
466 inhibition, the restriction enzyme site for XhoI was sequenced with the forward primer for *accA.*
467 We flanked the restriction enzyme NcoI to the reverse primer for *accA.* We amplified the
468 antisense DNA sequence for the *accA* gene through PCR. The PCR product would become
469 inverted when inserted into the IPTG-PT-asRNA inducible pHN1257 plasmid, forming
470 recombinant DNA plasmids for asRNA transcription in vitro. The transformed competent
471 bacterial cells expressed the antisense RNA, and we extracted the RNA for qPCR analysis of the
472 *accA* gene. The primers for the *luxs* gene were applied to quantify the number of gene copies
473 from qPCR analysis for cells grown in glucose enhanced samples. We used the primers for the
474 *accA* gene for the quantification of the *accA* gene from the samples cultured with an increasing
475 gradient of glucose solutions.

476 The total RNA concentration for the control, (-) asRNA, equaled 739.44 ng/µL. The
477 control, (-) asRNA, yielded a miRNA concentration of 334.98 ng/µL (Fig 4). The RNA
478 concentration for transformed bacterial cells with the asRNA of *accA* pHN1257plasmid was
479 279.28ng/µL. The miRNA concentration of the cells with asRNA measured to 240.90 ng/µL.
480 The gene of *accA* was successfully suppressed by asRNA in vitro with 63 ng/ µL of the qPCR
481 measured for bacteria cells (n=3) transformed with the recombinant antisense pHN1257 plasmid
482 DNA (37.8 ± 35.6). The real-time PCR results for the bacterial cells without the antisense gene
483 target and insert yielded 421.69 ng/µL for *accA* (Fig 5). There was a 147 % difference between
484 cells not expressing asRNA versus cells transcribing the asRNA for *accA* (p=0.027). Inhibiting
485 or lessening ACCase activity limits the synthesis of lipids, causing many physical changes.
486 Antisense RNA expression can modify the consistency of fatty acids by upregulating the
487 production of the ACCase enzyme.

488

489 **Figure 4 RNA Concentrations vs. Glucose Concentration** A) The enhanced *E. coli* bacteria
490 cultures (n=3) with 200µM, 50µM, and a control of glucose (59±49). B) The 50µM of glucose in
491 a bacterial sample highest yield was 566ng/µL, for 200µM 117ng/µL of RNA was produced, and
492 the control measured to 76ng/µL of RNA.

493 A)

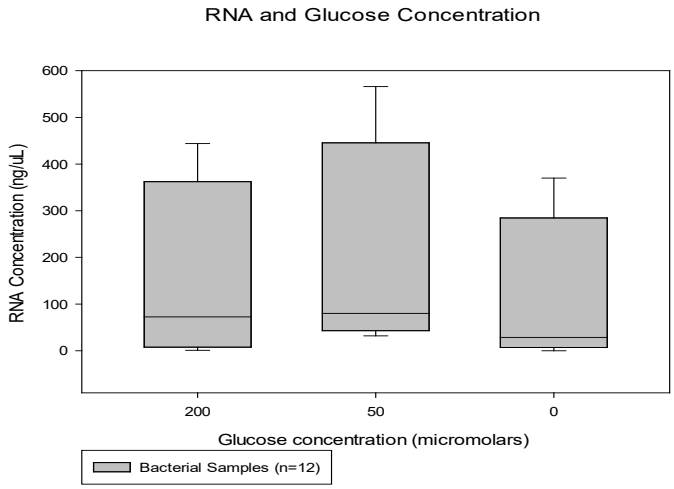

494

495 B)

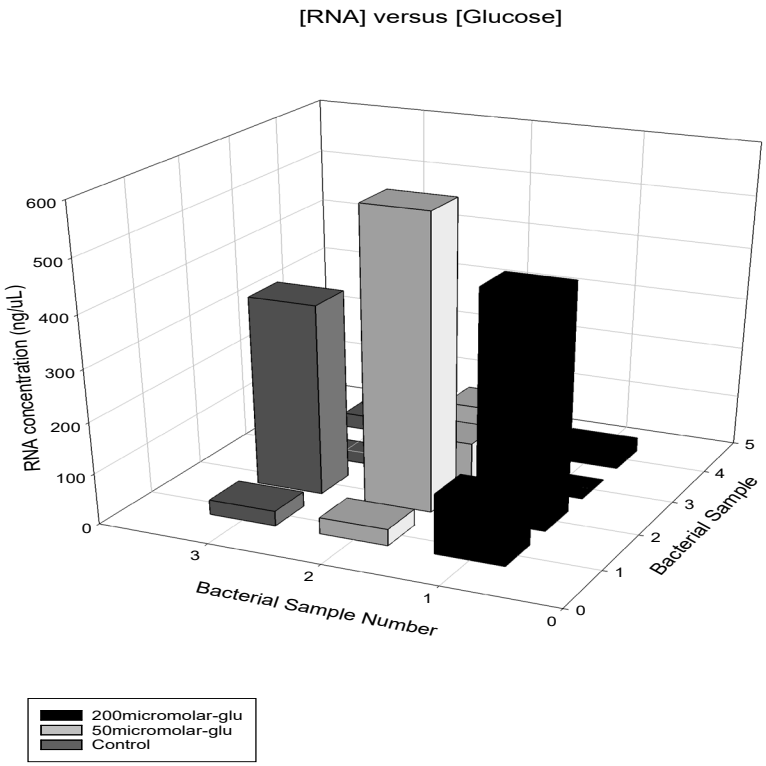

496

497

498 **Figure 5 The qPCR results for quantifying *accA* concentration and the gene copy number.**

499 The RNA for each sample, 15mM, 7.5mM, 5mM, and the control, was reverse transcribed into
500 the first-strand cDNA, and absolute quantification with qPCR was used to measure the amount
501 of the target gene, *accA,* produced by each sample. A) High glucose had a Cp of 12.28, and the
502 concentration of *accA* was 4.21E3 ng/µL. The Cp of sample medium-glucose equaled 16.51 with
503 a concentration of 3.75E2, and the low-glucose Cp was 14.08 with a target gene concentration of
504 1.50E3. B) The gene of *accA* was successfully suppressed by asRNA in vitro, with 63 ng/µL
505 measured for bacteria cells transformed with the recombinant antisense pHN1257 plasmid DNA.
506 The bacterial cells with the pHN1257 plasmid but without the antisense gene target and insert
507 produced 421.69 ng/µL for *accA.* There was a 147% percent difference between cells not
508 expressing asRNA versus the cell transcription of the asRNA for *accA* (p=0.027).

509 A)

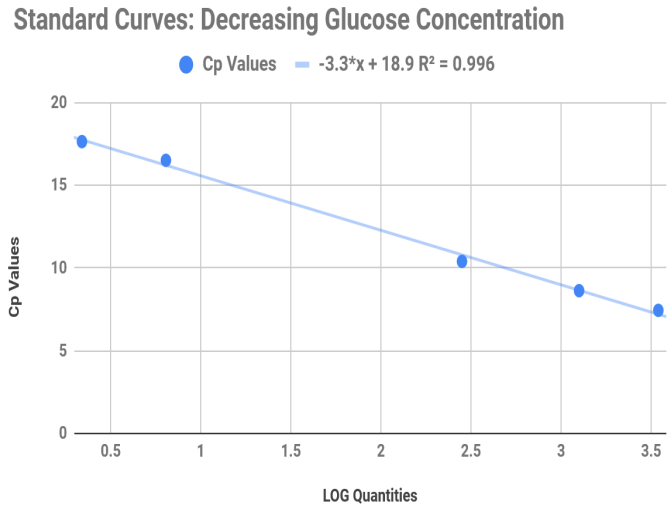

510

511 B)

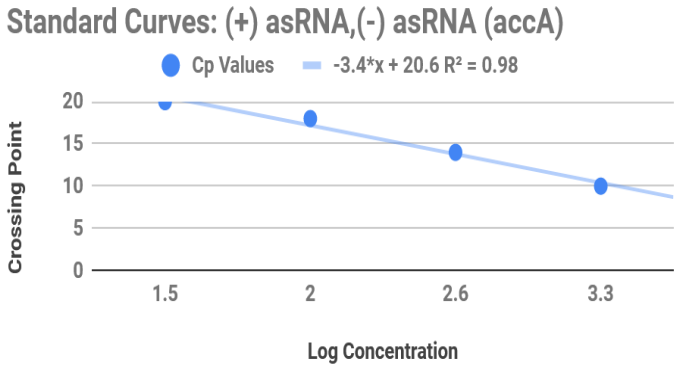

512

513

514 During short-chain fatty acid synthesis, malonyl-CoA is formed from acetyl-CoA, using
515 energy from ATP and bicarbonate production [23]. The hydrolysis of glucose produces two
516 pyruvates. The pyruvates alter into acetyl-CoA, forming acetate (Table.3). Through the Wood-
517 Ljugdahl pathway, pyruvate loses two hydrogens, carbon dioxide loses oxygen, altered into
518 carbon monoxide, and a methyl group is added to the oxidation, synthesizing acetyl-CoA into
519 Acetate [28]. The production of butyrate occurs when two molecules of acetyl-CoA combine into
520 acetoacetyl-CoA. The transformation of acetoacetyl-CoA into butyryl-CoA produces butyrate
521 [25]. The succinate or acrylate pathway composes the propionate [29]. The
522 phosphoenolpyruvate, or PEP, is broken into pyruvates that metabolize with water to produce
523 succinate. The succinate is reduced into propionyl-CoA, forming propionate (Table. 3). Through
524 the acrylate pathway, lactate loses oxygen, forming propionate [28].

525 **Table 3 Pathways for Biosynthesis of SCFAs from Carbohydrate Fermentation**

Glucose	Glucose	Glucose
2 Pyruvates Lose a Hydrogen	2 Pyruvates Lose a Hydrogen	2 Pyruvates Lose 1 Hydrogen Gain 1 Hydrogen
Acetyl CoEnzyme A	Acetyl Coenzyme A	LACTATE Loses 1 Oxygen
B-hydroxybutyryl CoA Lose H2O	Phosphate Replaces The CoA	Creates Acryloyl-CoA
Crotonyl CoA Gains a Hydrogen	Creates Acetyl-Phosphate	Forms Propionyl-CoA
Butyryl CoA Phosphate Replaces The CoA	Phosphate added to ADP to make ATP	CoA in Propionyl-CoA Replaced with a Phosphate
Butyryl Phosphate formed The Phosphate moves to an ADP to form ATP **BUTYRATE**	**ACETATE**	Phosphate removed **PROPIONATE**

526 **For synthesis of each SCFA, glucose is hydrolyzed into 2 molecules of pyruvate, which then**
527 **lose a hydrogen, forming Acetyl Coenzyme A**. For butyrate the Acetyl coenzyme A loses a
528 water, forming B-hydroxy butyryl CoA, where it loses a hydrogen, and the CoA is replaced with
529 a Phosphate causing the removal of the phosphate. After the loss of the phosphate yields the
530 butyrate. Acetate forms when a phosphate group replaces the CoA in Acetyl Coenzyme A, and
531 then the phosphate added to an ADP produces ATP. Propionate can form when lactate loses
532 oxygen, giving Acryloyl-CoA, to convert into Propionyl-CoA that replaces the CoA with
533 phosphate, and then removed by a kinase to produce propionate.

When the ACCA subunit of ACCase transfers a carboxyl group to acetyl-CoA, converting into malonyl-CoA, the malonyl-CoA catalyzes the synthesis of the LCFAs (Fig 6). The fatty acid cycle synthesizes long chains of fatty acids for the formation of the bacterial plasma membranes and a thin-layered matrix for initial bacterial attachment to a biotic or abiotic surface. After bacteria attach to a surface, more growth occurs until a microcolony of bacterial cells form, and the gene *accA* codes for the subunit of the Acetyl-CoA Carboxylase complex. Acetyl-CoA carboxylase (ACC) initiates the first step of fatty acid synthesis. An acyl-group or an ACP is added to the malonyl-CoA and converted into a ketoacyl-ACP. The Beta-ketoacyl-ACP is reduced, gains hydrogen, into Beta-hydroxyacyl-ACP. The Beta-hydroxyacyl-ACP is dehydrated, losing a molecule of water, to alter into an Enoyl-ACP, which forms into an Acyl-ACP by gaining two hydrogen protons.

Figure 6 Long-Chain Fatty Acid Synthesis An acyl-group or an ACP is added to the malonyl-CoA and converted into a ketoacyl-ACP. The Beta-ketoacyl-ACP is reduced, gains hydrogen, into Beta-hydroxyacyl-ACP. The Beta-hydroxyacyl-ACP is dehydrated, losing a molecule of water, to alter into an Enoyl-ACP, which forms into an Acyl-ACP by gaining two hydrogen protons.

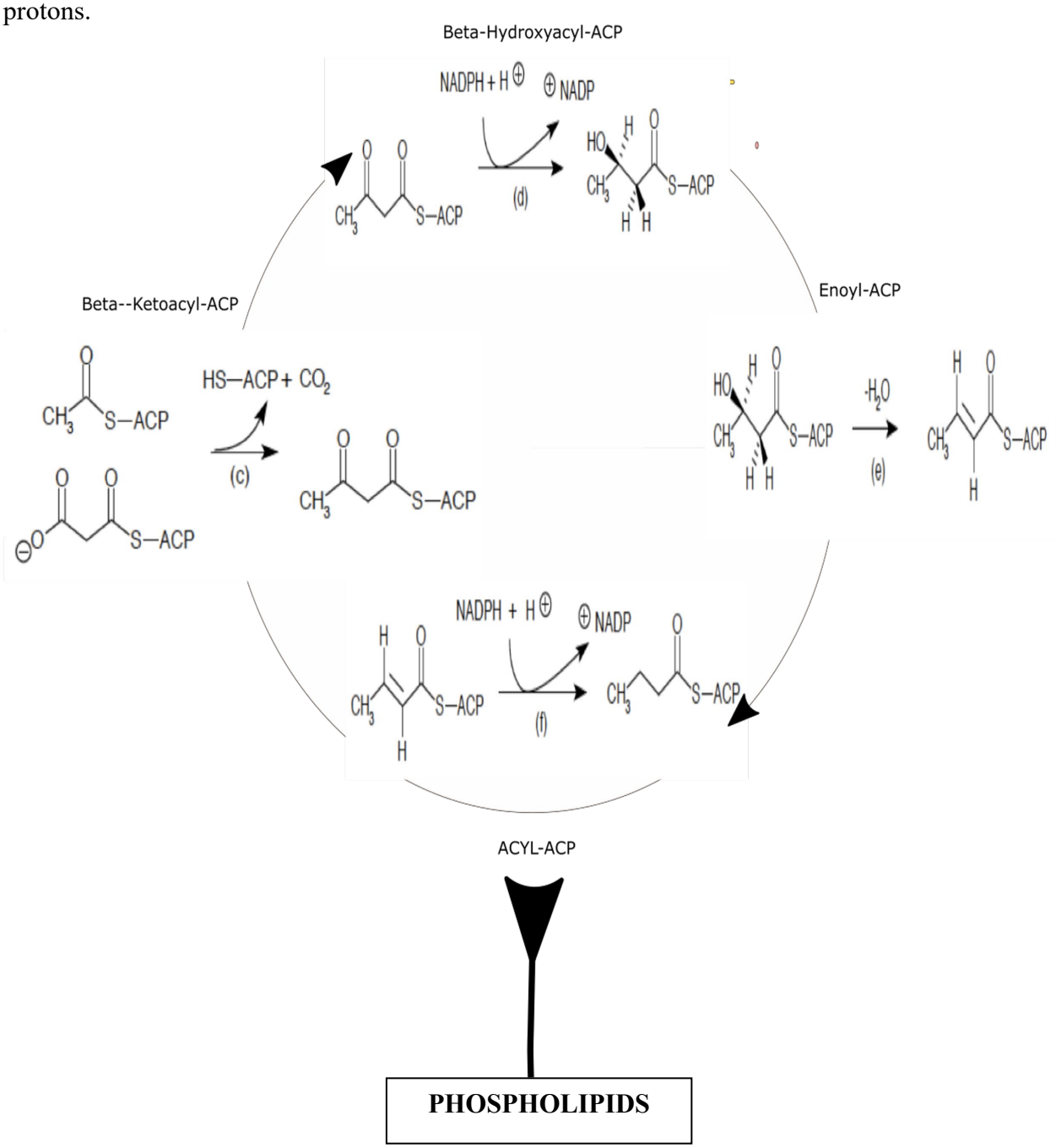

572 **QUANTIFICATION OF LUX-S GENE EXPRESSION**

573 The gene *accA* is a component of the ACCA subunit of the ACCase complex, which
574 functions as a transferase. The ACCA subdomain of ACCase is vital for catalyzing fatty acid
575 synthesis. Lipid biosynthesis is responsible for increased quorum sensing and biofilm formation.
576 After the hydrolysis of glucose into two pyruvate molecules, the alpha subunit, ACCA, transfers
577 a carboxyl group to acetyl-CoA to produce malonyl-CoA. The malonyl-CoA enters the lipid
578 biosynthesis pathway. The fatty acids produced to assist with secreting a more fluid membrane,
579 stretching the span of the biofilm matrix. As the biofilm matrix expands the microcolonies of
580 bacteria grow proportional to the size of the matrix. The increase in the number of colonies
581 induces the release of autoinducers, which accrue into a display of bioluminescence. The
582 bioluminescence is a signal of quorum sensing. The gene *luxs* is needed to produce autoinducer-
583 2. *luxs* monitors the amount of biofilm, flagellum movement, and regulates the factors of
584 virulence. The ACCA subunit catalyzes the synthesis of lipids required for inducing the release
585 of AI-2 that are signals produced during quorum sensing.

586 The high levels of autoinducers initiate a positive feedback loop, switching all bacterial
587 cells into producing quorum signals that create a bioluminescence [25]. The autoinducers
588 compile in the surrounding environment of a bacterial cell as the bacterial population increases
589 [11]. The bacteria sense the growth in the population and begin tracking the changes in the
590 number of cells, which help to change the amount of genetic expression [30]. Quorum sensing
591 between bacterial cells monitors the genes responsible for organizing the activities executed by
592 different bacterial groups. Activities completed through quorum sensing include
593 bioluminescence, spore formation, antibiotic excretion, creating a biofilm, and releasing factors
594 for virulence [11]. Biofilm can increase the movement of pathogenic bacteria into the
595 bloodstream [13].

596 Therefore, there can exist a significant link between bacterial cell metabolism and
597 virulence. By quantifying the measurement of gene copies for *luxs* while inhibiting *accA* with
598 asRNA, the connection of metabolism with pathogenesis could be demonstrated (Fig 7).
599 *Escherichia coli* cells were grown in 25µM and 5µM of glucose and transformed with antisense
600 pHN1257expressing IPTG-PT-asRNA plasmids. Cell samples with 5µM glucose- (+) asRNA
601 produced a high measure of the *luxs* gene. The gene copy number of *luxs* for (+) glucose/ (+)
602 asRNA, and (+) asRNA were quantified. For the results, the (-) glucose-(+) asRNA sample
603 produced a gene copy number of 199 and 2511 *luxs* copies for (-) glucose- (-) asRNA (n=3, 277
604 ± 37). For the 25µM glucose-(+) asRNA and 5µM glucose (+), asRNA produced 39,810 and
605 316,228 gene copies of *luxs*, respectively (Fig 8). The control samples, the (-) glucose-(-)
606 asRNA, (n=3, 658,114 ± 483,499) and the 5µM glucose- (+) asRNA (n=3, 171571±204574)
607 exhibited the highest amount of expression for *luxs* with a $p<0.05$ ($p=0.025$) (Fig 8). Table 4
608 displays the ANOVA results of the qPCR gene copies for the *luxs* gene.

609

610

611

612 **Figure 7 Gene Copies for *luxs* determined through the qPCR measurement**

613 The qPCR procedure measured the number of gene copies for *luxs* A) (-) glucose-(+) asRNA
614 sample had a gene copy number of 199. B) There were 2511 *luxs* copies for (-) glucose-(-
615)asRNA. The 5µM glucose-(+) asRNA yielded 316,228 gene copies of *luxs* D) The 25µM
616 glucose-(+)asRNA produced 39,810 gene copies.

617 **A)** **B)**

618

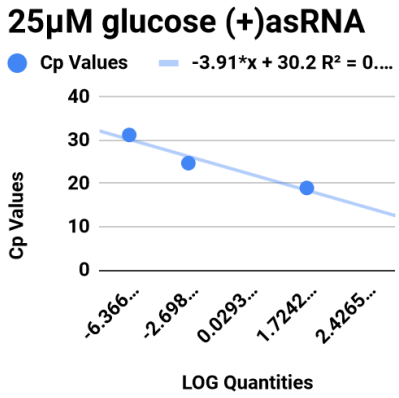

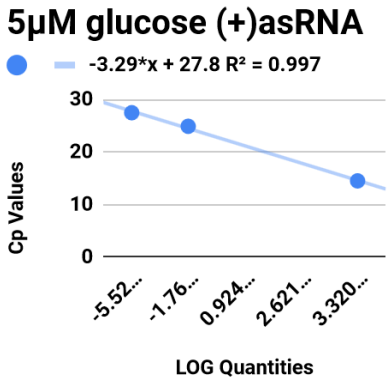

619
620

621 **C)** **D)**

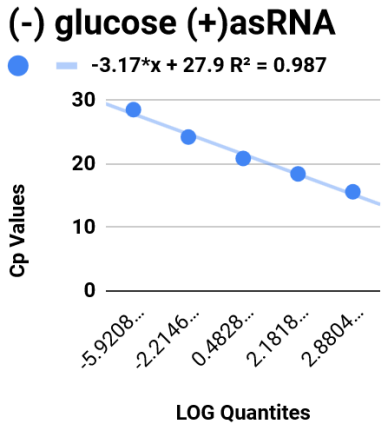

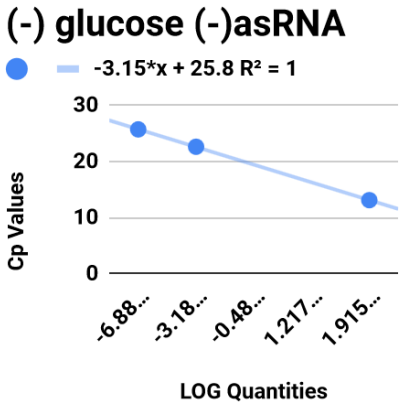

622
623

624

625

626

Figure 8 The Total Production of *luxs* versus the Control Sample. The polar plot compares the control sample for the qPCR quantification of the gene *luxs* after exposure to glucose and antisense RNA in the form of the pHN1257-IPTG-asRNA expression plasmid. A) The control compared to the asRNA sample, to the 25micromolar-glu-asRNA sample, and versus the 5µM-glu-asRNA sample equaled the following polar coordinates (radius, theta): ($1x10^6$, 180º), ($5x10^5$, 60º), and ($6x10^5$,68º), respectively. B) The control, 5, 25, and the asRNA micromolar samples production of the *luxs* gene are displayed in the 3D contour graph as an intense red, purple/blue for the 5µM-glu-asRNA, and purple for the asRNA including the 25µM-glu-asRNA sample. The control sample yielded a higher measure of *luxs* with $1x10^6$ gene copies (658,114 ± 483,499). The sample without glucose but with asRNA expression produced 199 gene copies of *luxs* (n=3, 277 ± 37).

A)

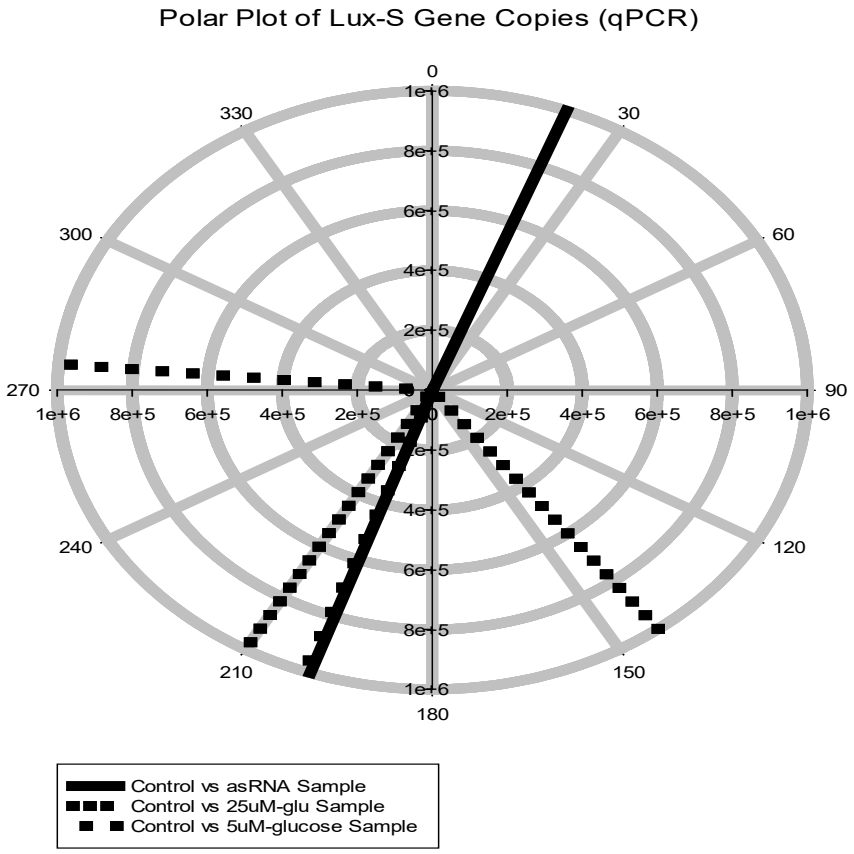

650
651
652 **B)**

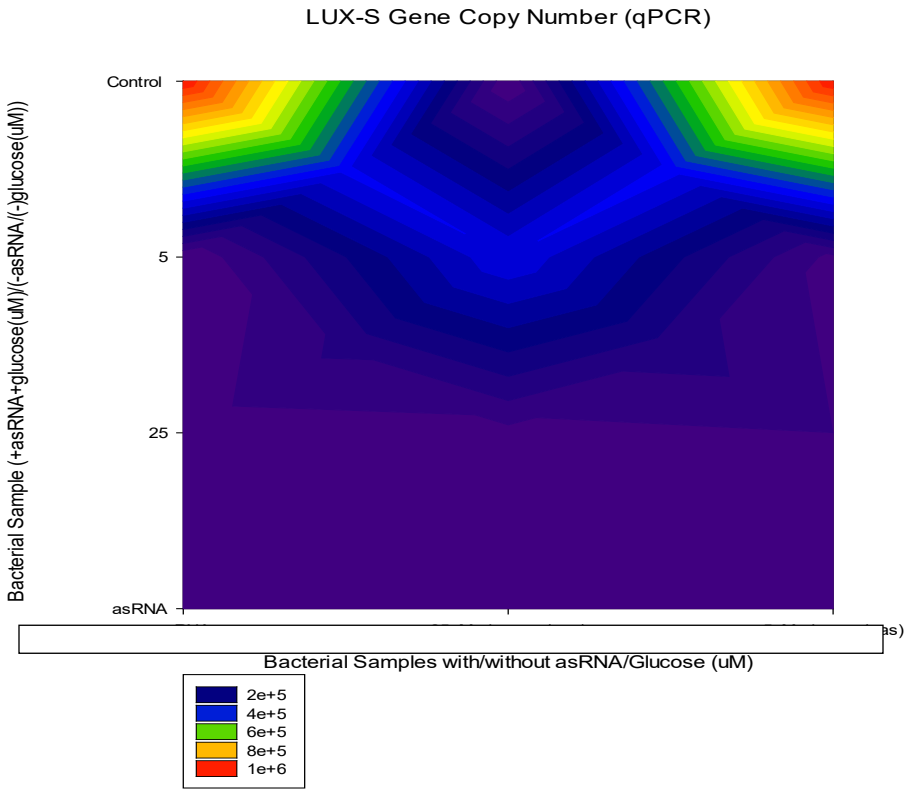

653
654
655
656
657
658
659
660
661
662
663
664

Table 4 ANOVA results for the total experimental sample for quantifying gene copies through qPCR

ANOVA Results of qPCR Gene Copies

	luxs-glu/ (+) asRNA	*luxs*-glu/ (+) asRNA	(-)glu(-)asRNA	*acc A* (-) asRNA (+) glu/ (-) glu	*accA* (+) asRNA (+) glu/ (-) glu
1	2511	316228	1000000	186	100
2	2000	26915.4	1000000	79	32
3	741	17783	39810	18	5
4	199	251	151286	7.4	3
n	4	4	4	4	4
X	1363.750	90294.350	547774.000	72.600	35.000
s	1074.010	151028.260	524165.009	81.920	45.306

X_{ave} 127907.940

total	19	1798315304447.08

source	df	SS	MS	F	P-value
treatments	4	905636341810.108	226409085452.527	3.8044	0.0250
error	15	892678962636.940	59511930842.463		
total	19	1798315304447.04			

ANOVA Results of qPCR Gene Copies the ANOVA results reveal an overall mean of 127907.940 for the total number of trials that yielded a total and a sum of gene copies through Real-Time PCR absolute quantification. The sample without glucose and antisense RNA, (-) glucose-(-)asRNA, produced the highest amount of gene expression, for *luxs* and *accA* with 547774.000 as a mean of the total number of gene copies yielded from the qPCR analysis (p=0.025).

672 The 5µM glucose- (+) asRNA sample expressed more of the *luxs* gene than the 25µM
673 sample. Wang et al., (2005) found that adding 0.8 percent glucose to their bacterial culture and
674 growth medium increased the activity at the promoter site of the *luxs* gene. A glucose
675 concentration of 5µM results in a normal exogenous osmolarity surrounding bacterial cells
676 within the microflora in the gut of the lower digestive tract [31]. We expected the overly
677 saturated cells at 25µM to elevate the gene expression of *luxs.* However, the excess saturation of
678 glucose at 25µM did not result in the amplified gene expression of *luxs*. Jesudhasan et al. (2010)
679 proved that higher levels of autoinducer-2 did not lead to the increased gene expression of *luxs* in
680 *Salmonella typhimurium* when cultured in high concentrations of glucose [29].

681 Glucose affected the rate of transcription, increased the production of nucleic acids, but
682 the inhibition of *accA* with asRNA significantly suppressed gene expression. From the control to
683 the 25 µM glucose exposure, bacteria cells transcribed DNA at an amplified rate (Fig 9). As the
684 glucose concentration increased to 50 µM, the rate of transcription reached a sustained
685 equilibrium with no new nucleic acid production or activity as the concentration approached 200
686 µM. The samples expressing asRNA inhibition of *accA* produced 16% of the total yield of
687 nucleic acid. Samples not expressing asRNA inhibition yielded 83% of the total quantity of
688 nucleic acid.

689 Moreover, by transforming *Escherichia coli* bacterial cells with IPTG-PT-asRNA
690 inducible vectors, which targeted the gene *accA,* the gene expression of *luxs* gene also decreased.
691 Because glucose delays the movement of the *luxs* mutant strain with bacterial overpopulation but
692 does not inhibit bacterial growth, each (+) glucose- (+) asRNA bacterial colony appeared smaller
693 and defected. Osaki et al. (2006) showed that *luxs* mutants could be smaller in diameter with 8.0
694 mm versus 12.3 mm in its wildtype [32]. The bacterial colonies expressing antisense RNA
695 (5mm) were a smaller size versus cells without antisense RNA transcription (8mm) of *accA.* The
696 cell samples with (+) asRNA transcription were found by many previous research studies to
697 appear smaller in size[23].

698 Bacterial samples transformed with IPTG-PT-asRNA inducible pHN1257 plasmids and
699 designed to inhibit the *accA* gene displayed the least measure of *luxs* expression. The (-) glucose-
700 (+) asRNA sample exhibited the lowest amount of *luxs* expression of 199 gene copies (225 ±
701 37). As a result, the mutated *luxs* gene exhibits less expression that causes the biofilm to appear
702 thinner, looser, and displaying an appearance of bacterial cells with defects. Lux-S forms a
703 thicker and more viscous biofilm, which is a result of many nucleic acids released into the
704 extracellular matrix of the biofilm.

705

706

707

708

709

710 **Figure 9 The effect of glucose on the rate of transcription, inhibition with asRNA, and the**
711 **frequency of Nucleic Acid production.** A) From the control to the 25 μM glucose exposure,
712 bacteria cells transcribed DNA at an amplified rate. As the glucose concentration increased to 50
713 micromolar, the rate of transcription reached a sustained equilibrium with no new nucleic acid
714 production or activity. B) The asRNA caused the gene inhibition of *accA.* The samples
715 expressing asRNA inhibition of *accA* produced 16% of the total yield of nucleic acid. Samples
716 not expressing asRNA inhibition yielded 83% of the total quantity of nucleic acid.

717
718 **A)**

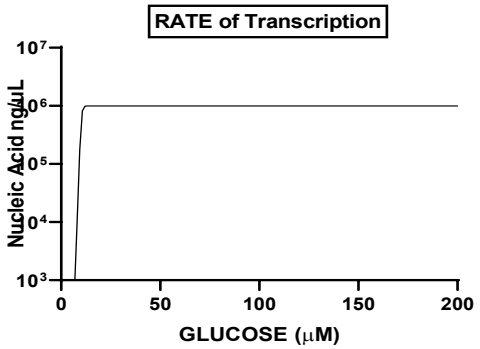

719
720 **B)**

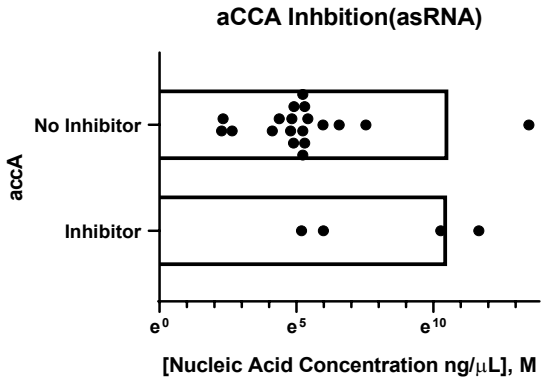

721

722 The ample amounts of DNA are released to maintain a more solid macromolecular matrix
723 and consistency of the biofilm [33]. Lux-S is required for AI-2 production and for regulating
724 gene expression in the early-log-growth phase. Pathogenic bacteria depend on biofilm formation
725 to attach to epithelial cells and tissues, spreading infectious diseases. Pathogenic bacteria infect
726 host cells by accumulating AI-2, exogenously, which then increases the amount and consistency
727 of the formation of biofilm [34]. The gene *luxs* codes for the flagella complex, biofilm creation,
728 and controls virulent factors. The *luxs* gene, when it is more expressed, causes the spread of
729 virulent bacteria through increasing the motility and movement of pathogenic bacteria. More
730 Lux-S expression, as a result of mutations in the *luxs* gene, produces increased amounts of
731 biofilm, assisting pathogenic bacteria to invade the mucosal layers and the epithelial cells of its
732 host, developing into a systemic infection.

733 The autoinducer-2 that accumulates monitors cell growth by permitting bacterial cells to
734 sense the excess AI-2 and then terminate population growth. The excess AI-2 distributes quorum

735 signals between bacterial cells, which notifies cells of limited nutrients, surface area, or space.
736 Autoinducer-2 requires the genetic expression and translation of *luxs* (Fig 8). When Lux-S and
737 autoinducer-2 are less regulated and overexpressed, infectious bacteria can propagate in stressful
738 environments with high acidity and salinity [27]. Kendall et al. (2008) demonstrated the ability
739 of *S. pyogenes* to adapt to acidic conditions as a result of an unregulated Lux-S/AI-2 system [25].

740 The *Vibrio fischeri* process of quorum sensing differs drastically compared to the
741 *Escherichia Coli*. *Vibrio fischeri* synthesizes AI-2 through an enzyme called an autoinducer
742 synthase or the LuxI that produces a hormone class of acyl-homoserine lactones, AHL, which is
743 the autoinducer $3OC_6$-homoserine lactone. In *Vibrio fischeri*, the AHL binds to the autoinducer
744 receptor called Lux-R for initiating a transcriptional activator of DNA [35]. After AHL is
745 produced, it passes through the cell's plasma membrane as the number of bacterial cells
746 increases, and then it stops diffusing after cell density reaches a threshold. When the AHL is
747 attached to the LuxR complex, the operon is activated, transcribing the genes that code for the
748 enzyme luciferase [35]. The LuxR-AHL bond releases, into the periphery of the cell, high levels
749 of quorum sensing molecules that stimulate the cell to cell communication between bacteria
750 species [31].

751 The *Vibrio fischeri* process of quorum sensing immensely differs in comparison to
752 *Escherichia Coli* because *Escherichia Coli* and many gram-negative bacteria regulate the influx
753 and output of autoinducer-2. In *Escherichia Coli*, the transporter complex called LsrABCD
754 regulates the uptake of autoinducer-2. The repressor of LsrABCD and the LsR is a kinase that is
755 a part of the quorum-sensing system of AI-2. The cyclic AMP/cyclicAMP receptor proteins
756 regulate the lsr operon. The expression of cyclic AMP/cyclic AMP receptor proteins occurs with
757 the positioning of *lsrK* and *lsrR* upstream of the lsr [36]. Lsrk that is a kinase located in the
758 cytoplasm phosphorylates AI-2 that then attaches to the *lsr* repressor. The activated and attached
759 AI-2 suppresses the *lsr* repressor LsrR. After the activity of the *lsr* repressor is inhibited, the
760 release of AI-2 increases via the autoinducer-activated expression of the Lux-S protein.

761 The development of biofilm that initiates infection requires the activation of the luxs
762 gene. Its excessive amplification and expression form a denser texture of biofilm [33]. Lux-S
763 monitors virulence through regulation of the process for generating biofilm in the nasopharynx in
764 mice with pneumonia, *Streptococcus pneumoniae*. Flagella expression increases with *luxs*
765 mutation in the lungs and bloodstream. The *luxs* mutants can infect the lungs or the bloodstream
766 more rapidly than its wild-type strain [35]. Flagellin increases inflammation by activating Toll-
767 Like Receptor Signaling or TLR5 pathways, which translates pro-inflammatory genes within the
768 Mitogen-Activated Protein Kinase or the MAPK pathways. Flagella modulates virulence and
769 pathogenesis by allowing more rapid motility of bacteria, infecting the colonization of host cells,
770 and assisting infectious bacterial cells into entering the mucosal layers [37].

771 Pathogenic bacteria determine the level of autoinducer signals specific for their species.
772 Pathogenic bacteria require a specific order and assortment of virulent genes to cause infection.
773 For example, the different residues or R-groups of amino acids within autoinducers bind to the
774 LUXR protein receptors in a conformation specific to the amino acid side chains within the
775 binding sites. The orientation of the AI to protein receptor binding sites produces varied types of
776 side-chain lengths and amino acid substitutions [38]. For example, pathogenic bacteria as
777 Enteropathogenic *Escherichia coli* EPEC release intraspecies-type of signals that help to

778 colonize the small intestines because the small intestines are void of much commensal
779 microflora. The Enterohemorrhagic *Escherichia coli* or EHEC pathogenic form of *Escherichia*
780 *coli* conducts signals with other diverse bacterial cell types and with host cells. The EHEC
781 communicates through quorum sensing with other colonic bacteria cells. The EHEC infects
782 epithelial cells through activating the genes called the Locus of Enterocyte Effacement or LEE.
783 The genes of LEE are required for A/E lesions to form when EHEC cells attach to and efface
784 from epithelial cells, amplifying the level of pathogenicity [35].

785 When the production of Lux-S is blocked, the intensity of disease-causing bacteria
786 changes. For example, the mutation of *luxs* in *the Haemophilus influenzae* increases virulence
787 that causes middle ear infections [39-Vidal]. The *A. pleuropneumoniae* and *M. haemolytica*
788 bacteria have autoinducer mutations that lessen virulence in mouse models. When inhibiting the
789 *luxs* gene, a reduction of pustule-creation occurs as compared to the parental wild type strain
790 [39]. However, autoinducer 3 is not dependent on the expression of the *luxs* gene. The *luxs*
791 genetic mutants impede the production of AI-3 [22-24]. As a result, the pathogenic Escherichia
792 coli, EHEC, collects signals from host cells in the form of hormones known as epinephrine. The
793 AI-3 can communicate with the transmembrane protein of the host cell called Qsec [40]. The two
794 components for quorum sensing also include Las and RhI that are quorum systems consisting of
795 activator proteins. The activator proteins direct the synthesis of the autoinducers. The proteins
796 called Las and RhI turn genes on or off based on the density of bacterial populations, sensing the
797 accumulation of autoinducers [41].

798 The bacteria called *P. aeruginosa* secretes two types of autoinducers called N-3-
799 oxododecanoyl, a homoserine lactone, (3-oxo C12-HSL), and N-butyryl-L-homoserine lactone
800 (C4-HSL). These autoinducers released can cause virulence in people infected by *P. aeruginosa*
801 by supplying virulent factors that help colonize and spread the infection [41]. Therefore, the
802 results present significant data for the effect of glucose and genetic inhibition of *accA* on the
803 production of the *luxs* gene, an essential component of bacterial virulence. The data demonstrates
804 that the genetic changes, as inhibiting the *accA* gene with antisense RNA, and the availability of
805 nutrients such as glucose, affected the production of *luxs*. Inhibition of the *luxs* gene can reduce
806 biofilm formation and decelerate the motility of bacteria, and then the lessened motility can
807 impede the spread of pathogenic bacteria.

808 **ANTIBIOTIC RESISTANCE TEST**

809 An antibiotic resistance test was performed to determine the susceptibility of antibiotics
810 from bacterial samples expressing antisense RNA inhibition of the gene *luxs.* The bacterial
811 samples expressing the pHN1257-asRNA-*accA* gene suppression were predominantly
812 susceptible to the antibiotic's tetracycline, carbenicillin, and chloramphenicol. Disks (N=64)
813 consisting of each of the three antibiotics were placed unto agar plates divided into 8 sections
814 (Fig 10). The zone of inhibition was measured in millimeters (Fig 11). For the experimental
815 group (with asRNA) the median was 20 mm for the measurement of the zone of inhibition.
816 Control groups (without asRNA) were mainly resistant to the antibiotics with a median of 6 mm
817 (Table. 5). A zone of inhibition or ZOI that measures less or equal to 14 for the tetracycline
818 antibiotic disks is considered resistant. The ZOI between 15-18, equal to, or greater than 19, are
819 intermediate or resistant to tetracycline, respectively. For chloramphenicol, a ZOI equal to/less
820 than 12, between 13-17, and equal to/less than 18 indicates resistance, intermediate

821 susceptibility, and susceptibility. The antibiotic carbenicillin demonstrates resistance,
822 intermediacy, and susceptibility at ZOIs of less than or equal to 19, between 20-22, and greater
823 than or equal to 23, respectively. Bacteria transformed with pHN1257-(+)asRNA-*accA* were
824 more susceptible to the antibiotic's tetracycline, carbenicillin, and chloramphenicol. Fifty-nine
825 percent of the experimental (+)asRNA-*accA* samples were sensitive to tetracycline,
826 chloramphenicol, and carbenicillin (21±4, SEM=0.7). The (+)asRNA-*accA* treatment group
827 displayed an intermediate sensitivity of 28% as 3% were resistant to antibiotics (13.75±10,
828 SEM=1.8). The control exhibited more resistance with 25%, 12.5%, and 53% of susceptibility,
829 intermediate, and resistance, respectively. The (+)asRNA-*accA* treatment group had an 82%
830 percent difference in susceptibility compared to the (-)asRNA-*accA* control group. The control
831 group showed a 77% difference in resistance when compared to the (+)asRNA-*accA*
832 experimental group (p=0.000554). A paired t-test was performed yielding a t-score of 3 and the
833 degrees of freedom equaling 31. The t-score and the DF were used to calculate the p-value.

834 The bacteria of *S. Aureus* translate a lysine at its 164th genomic position, forming an *S.*
835 *Aureus* that is resistant to the antibiotic called thailandamide. The thaillandamide also denatures
836 and deactivates the acetyl-CoA carboxylase enzyme with the ACCA transferase subunit. The
837 bacterium of *Salmonellae* also produces a mutation of the gene for *accA*. Other antibiotics as
838 capistruin and malleilactone are novel synthetic antibiotics that inhibit the transformation process
839 between bacterial cells. This blockage of bacterial transformation causes more production of
840 antibiotics. Another antibiotic called bactobulin can bind to and inhibit luxI-luxR proteins that
841 enable bacterial cell to cell communication through quorum sensing [42]. A molecule is released
842 that blocks ribosomal bacterial translation when the LuxI-R binds to the bactobulin. The
843 capistruin impedes RNA transcription by blocking the activity of RNA polymerase. The
844 malleilactone affects the release of quorum sensing molecules. Therefore, there is a need for
845 designing the types of novel bacterial antibiotics that can target the metabolic processes of
846 pathogenic bacteria. It is possible to conjoin the genetics that signal and regulate metabolic
847 processes with antibiotic development. The metabolic processes of bacteria exhibit a strong
848 complementary relationship with antibiotic resistance.

849 The bacterial uptake of antibiotics increases when the metabolic processes are regulated.
850 The element of carbon alone serves to induce the degradation of pathogenic bacteria by
851 amplifying antibiotic sensitivity. When carbon is present in the extracellular matrix of bacteria,
852 an increase in the protonmotive force or PMF increases with more NADH activity. The TCA
853 cycle is activated during the raised activity of NADH and PMF. For example, A new bacterium
854 called *V. natriegens* was used to quantify the effects of the influx and changes of glucose
855 molecules on bacterial metabolism. The measurements occurred during the exponential growth
856 stage of *V. natriegens*. Researchers labeled glucose molecules with Carbon-13. They collected
857 the data and fitted the results of the concentrations of acetate, the RNA ribose sugars, and the
858 Carbon-13 labeled glucose to a graphical linear regression model.

859 They found that there was an elevated level of glyosidic activity at 80± 0.5 and the
860 activity of phosphoglucose isomerase combined with glyceride 3-phosphate dehydrogenase
861 action increased with a standard deviation of 169 ± 1. There were also many alterations
862 demonstrated in the TCA cycle with a standard deviation of 17 ± 1 for the synthase of citrate and
863 for ketoglutarate a standard deviation of 7 ± 0.4 was measured [43]. The *V. natriegens* showed
864 that 50% of its energy, from glucose altered into ATP, was donated to the process of glycolysis

865 that aided the TCA cycle to produce 40% more energy. *V. natriegens* can also be used like *E.*
866 *coli* for cloning procedures that study the genetics of bacterial metabolic genes. Like *E. coli*, *V.*
867 *natriegens* use their energy from ATP production through the TCA cycle to proliferate its cells,
868 regulate its homeostasis, and to transport its metabolites as substrates. A test based on a list of
869 criteria for antibiotic resistance is also needed to measure and diagnose antibiotic resistant
870 bacteria in the environment [44]

871 **TABLE 5 Antibiotic Resistance Test and the Diameter of the Zone of Inhibition**

TET[1]- (+)asRNA-*accA* **[2] **ZOI[3] (mm)**		**TET- (-)asRNA-*accA* ***[4]** **ZOI (mm)**	
21	**S[5]**	**21**	**S**
17	**I[6]**	**24**	**S**
17	**I**	**20**	**S**
20	**S**	**16**	**I**
21	**S**	**17**	**I**
19	**S**	**16**	**I**
20	**S**	**17**	**I**
18	**I**	**14**	**R[7]**
Carb[8]- (+)asRNA-*accA* **ZOI (mm)**		**Carb- (-)asRNA-*accA*** **ZOI(mm)**	

[1] Tetracycline
[2] **= Mean (21), SD(4), & SEM(0.7)-antisense
[3] ZOI=Zone of Inhibition
[4] ***=Mean (14), SD(10), & SEM(1.8)-control
[5] S=Susceptible
[6] I=Intermediate
[7] R=Resistant
[8] Carbenicillin

19,28	**R, S**	**29, 6**	**S, R**
21,21	**I, I**	**6,6**	**R, R**
20,23	**I, S**	**6,31**	**R, S**
17,22.5	**R,**	**6,29**	**R, S**
21,35	**I, S**	**35,6**	**S, R**
23,27	**S, S**	**6,6**	**R, R**
22,25	**S, S**	**6,29**	**R, S**
26,28	**S, S**	**34,6**	**S, R**
Chlor[9]- (+)asRNA-*accA* ZOI (mm)		**Chlor- (-)asRNA-*accA* ZOI(mm)**	
17	**I**	**6**	**R**
15	**I**	**6**	**R**
20	**S**	**6**	**R**
18	**S**	**6**	**R**
18	**S**	**6**	**R**
19.5	**S**	**6**	**R**

[9] Chloramphenicol

20	**S**	**6**	**R**
18	**S**	**6**	**R**

872 **Antibiotic Resistance Test and the Diameter of the Zone of Inhibition** The zone of inhibition
873 was measured in millimeters. Bacteria cultured in LB broth were pipetted unto the plates and
874 spread with a sterile swab. The diameter of ZOI that produced no bacterial growth encompassing
875 the antibiotic disks were measured. Disks that contained tetracycline, carbenicillin, and
876 chloramphenicol were placed unto nutrient agar plates. The data collected for the zone of
877 inhibition was compared to an antibiotic resistance chart to determine the antibiotic susceptibility
878 of bacteria expressing asRNA for the gene *accA.* Bacteria transformed with pHN1257-
879 (+)asRNA-*accA* were more susceptible to the antibiotic's tetracycline, carbenicillin, and
880 chloramphenicol. Fifty-nine percent of the experimental (+) asRNA-*accA* samples were sensitive
881 to tetracycline, chloramphenicol, and carbenicillin (21±4, SEM=0.7). The (+) asRNA-*accA*
882 treatment group displayed an intermediate sensitivity of 28% as 3% were resistant to antibiotics
883 (13.75±10, SEM=1.8). The control exhibited more resistance with 25%, 12.5%, and 53% of
884 susceptibility, intermediate, and resistance, respectively. The (+) asRNA-*accA* treatment group
885 had an 82% percent difference in susceptibility compared to the (-)asRNA-*accA* control group.
886 The control group showed a 77% difference in resistance when compared to the (+) asRNA-*accA*
887 experimental group (p=0.000554).

888

889

890

891

892

893

894

895

896

897

898

899

FIGURE 10 Zone of Inhibition for Antibiotic Susceptibility Test Bacteria that were transformed with pHN1257-(+)asRNA-*accA* showed more susceptibility to the antibiotic disk, containing tetracycline, chloramphenicol, and carbenicillin. Twenty-seven of the total 64 samples were susceptible antibiotics. Eighteen of the samples were resistant as 13 were only intermediate. The ratio of (+)asRNA-*accA* to (-)asRNA-*accA* equaled 3:2. B) Within the range of 20 to 22 mm of the ZOI for the (+)asRNA-*accA* expressing bacteria, the antibiotic susceptibility showed a density of 0.01515. The control displayed less susceptibility at a 20 to 30 mm ZOI with a density of 0.007.

A)

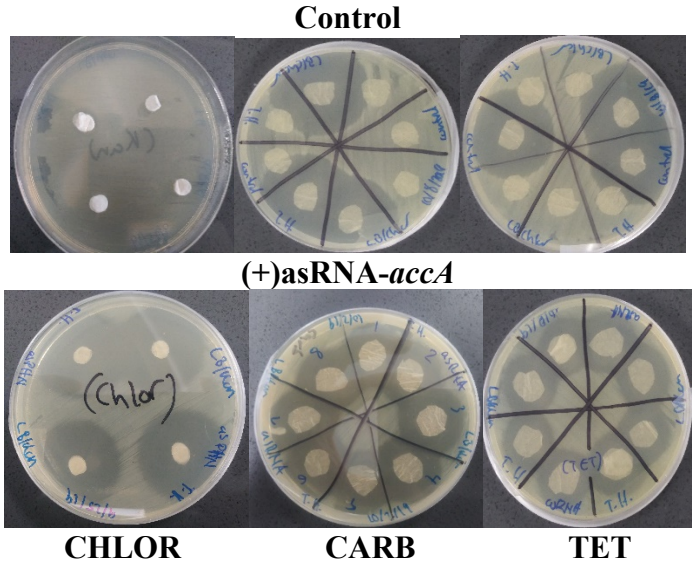

B)

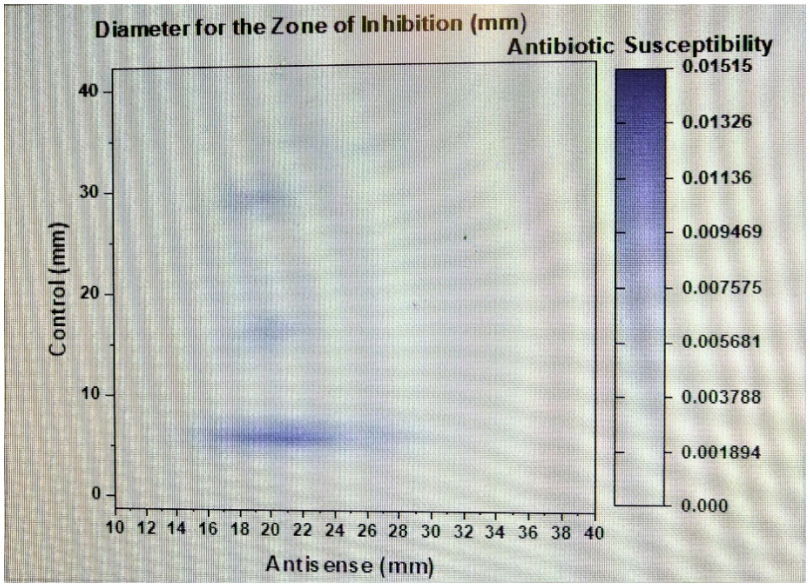

917 **CONCLUSION**

918 The overall purpose of the study was to confirm and identify the gene *accA* as a possible
919 target for blocking bacterial antibiotic resistance. Through examining the role of *accA,* a link
920 between bacterial cell metabolism and virulence was attempted and demonstrated. A cumulative
921 perspective, integrating bacterial cell metabolism via the ACCA subunit with bacterial
922 pathogenicity, may provide possible metabolic targets for designing new and potent antibiotics.
923 We reviewed in this study, an ability to design antibiotics that target bacterial cell metabolic
924 genes as *accA,* the binding sites of the ACCase enzyme, and the fatty acid synthesis pathway.
925 Cell metabolism can reduce the formation of bacterial cell biofilm needed for spreading
926 pathogenic bacteria by targeting the binding sites of the ACCase enzyme that limits the activity
927 of the fatty acid cycle. The potent condition of a bacterial population's metabolic state can
928 prevent bacterial susceptibility to antibiotics [16]. The results of decreased RNA expression and
929 cell growth in the presence of antisense RNA inhibition of *accA* may serve as a model for
930 blocking microbial metabolic processes that contribute to antibiotic resistance [45].

931 *Escherichia coli* cells were cultured in high glucose to a control concentration and
932 showed a decreasing range of gene expression for the target gene, *accA.* The observation of the
933 bacterial cells, grown in an increased amount of available glucose, showed the highest measure
934 of transcription for *accA.* The effect of glucose extracellular of the bacteria, on the concentration
935 of RNA, was measured by modulating the glucose concentration gradient. We determined the
936 level of transcription for the intracellular molecules as the *accA* gene through qPCR. The *accA*
937 gene was inhibited with antisense RNA, using an IPTG-inducible vector, pHN1257. There was a
938 138 percent difference in gene expression between cells transformed with antisense pHN1257
939 versus cells negative for antisense RNA during in vitro transcription. The re-engineered
940 pHN1257 plasmid expressed antisense transcription in vitro (Fig 1). Also, treating bacteria cells
941 that were transformed with asRNA for inhibiting *accA* demonstrated an increased bacterial
942 susceptibility to the antibiotics of tetracycline, carbenicillin, and chloramphenicol.

943 The constructed plasmid of PHN257 consisted of flanking inverted repeats for the target
944 DNA, rebuilding a paired double-stranded RNA terminus that inhibited the transcription of *accA.*
945 The qPCR results confirmed the inhibition of *accA.* The qPCR results yielded 63 ng/µL for *accA*
946 (+)asRNA versus 422 ng/µL for *accA* with (-)asRNA. The qPCR absolute quantification method
947 determined the total sum of gene copies for luxs. By increasing the glucose concentration in
948 increments, Wang et al. (2005) found that glucose increased the levels of autoinducer-2 of the
949 culture as well [46]. The observations displayed the RNA concentration for bacterial cells,
950 expressing asRNA of *accA,* included a concentration of 279.28 ng/µL. The miRNA
951 concentration of the cells with asRNA measured to 240.90 ng/µL.

952 Hydrolysis of a glucose molecule into two pyruvate molecules catalyzes the fatty acid
953 cycle. The acetyl-CoA Carboxyl transferase or the ACCA alpha subunit of the acetyl-CoA
954 carboxylase complex, AccABCD, transfers a carboxyl group from the pyruvate to the acetyl-
955 CoA to form malonyl-CoA. The malonyl-CoA enters the fatty acid synthesis pathway,
956 elongating fatty acids into long-chain fatty acids of phospholipids necessary for structuring
957 plasma membranes and for forming the initial extracellular matrix. The microcolonies attach,
958 aggregate, and accumulate in the extracellular matrix. As the colonies accumulate into large
959 populations, a release of autoinducer-2 molecules is triggered, causing certain bioluminescence

960 through an exchange of cell-to-cell quorum-sensing signals. The release of autoinducer-2 signals
961 cells to increase population growth or to preempt it. The release of AI-2 requires the gene
962 expression of *luxs*. The excess AI-2 distributes quorum signals between bacterial cells, which
963 notifies cells of limited nutrients, surface area, or space. If bacterial cells continue to accrue,
964 more biofilm is produced within the extracellular matrix, resulting in the dispersion of bacterial
965 cells. Biofilm is a potent virulent factor. Pathogenic bacteria can disperse from and cause a
966 systemic infection through excess biofilm production.

967 Also, the microflora can communicate with the host cells of the gastrointestinal tract
968 through a variety of chemical idioms [47]. A group of chemical molecules for bacterial language
969 expression and transfer includes homoserine lactones that are the most heavily studied. When a
970 bacterial infection occurs, homoserine lactones form and interrelate with the immune system
971 [48]. The rapid motility of spreading bacterial infection requires an increased release of quorum-
972 sensing signals that produce more biofilm. The production of biofilm induces resistance to
973 antimicrobial peptides. Biofilm maintains an intensive resistance to antibiotics as multi-drug
974 resistant pumps utilize biofilms for excreting antibiotics from bacteria. Mutations present in
975 genes that are a part of the metabolic pathway cause bacteria to become more susceptible to
976 antibiotic exposure.

977 The results supported the hypothesis. When decreasing the glucose concentration, while
978 suppressing the *accA* gene, led to an observed decrease in *luxs* expression. The author
979 hypothesized that decreasing the sum of glucose and suppressing *accA* gene expression would
980 decrease the expression of the *luxs* gene. The *luxs* gene is vital for quorum sensing and releasing
981 autoinducer-2. Increased expression of Lux-S produces more AI-2, which induces and initiates
982 quorum sensing between bacterial cells. The increased AI-2 molecules released triggers quorum
983 sensing for the amplified production of biofilm. Biofilm formation allows more pathogenic
984 bacteria cells to attach, proliferate, detach, and spread into a systemic infection. The bacteria
985 transformed with (+)asRNA-*accA*, for inhibiting *accA*, displayed antibiotic susceptibility to the
986 tetracycline, carbenicillin, and to the chloramphenicol. Targeting the *accA* gene, through its
987 inhibition, can increase the antibiotic sensitivity of resistant bacteria.

988 The *accA* gene translated into the acetyl-CoA carboxyl transferase enzyme transfers a
989 carboxyl group from pyruvate to the acetyl-CoA to form a malonyl-CoA. More glucose induces
990 more production of the acetyl-CoA carboxyl transferase. Increased glucose also causes more AI-
991 2 quorum-sensing signal molecules to accumulate. The malonyl-CoA enzyme is vital for
992 catalyzing the biosynthesis of long-chain fatty acids. The long-chain fatty acids are the building
993 blocks for biofilm formation. Therefore, a decrease of biofilm production can occur due to the
994 limited enzymatic activity of the ACCA transferase subunit via *accA* gene inhibition.

995 However, in the presence of glucose with antisense RNA transcription, *Escherichia coli*
996 cells continued to produce amplified amounts of *luxs* with 316,228 copies measured through
997 qPCR when enhanced with 5µM of glucose (n=3, 171571± 204574). The limitations of this
998 study include the contradictory results of the 5µM glucose-(+) asRNA sample for *luxs*. Adding a
999 5µM concentration of glucose to the LB broth culture increased the gene expression of *luxs*
1000 *during* the *inhibition of the accA* gene. These contradictory and unexpected results may show
1001 early signs of reduced efficacy of the inhibition of the *accA* gene in the presence of glucose.

The 5µM of glucose probably triggered increased expression in the *accD* gene and of the ACCD subunit, which was not inhibited by asRNA. The gene *accA* can continue to act as a potent metabolic target for suppressing antibiotic resistance. This study suggests that designing antibiotics could include targeting metabolic genes and enzymes. During the past 30 years, the formulation and discovery of potent antibiotics have dwindled [49]. However, there is a renewed focus for examining bacterial targets located in metabolic pathways. Zuberi et al. applied CRISPRi technology to inhibit the luxs gene in *E. coli* cells, and they found that biofilm formation depended upon the expression of luxs. They used Crystal violet to assess luxs effects on biofilm. Biofilm formation decreased as the expression of luxs was inhibited [50]. Hall et al. concluded that the cause of antibiotic resistance or the antibiotic sensitivity of biofilms may originate from a genetic source [51]. For future research, studying the gene expression, structure, and function of the ACCase complex needs further elucidation to design antibiotics that target bacterial-metabolic enzymes and genes.

ACKNOWLEDGMENTS

Special thanks are given to the staff from TheLAB in Los Angeles, CA. They were responsible for ordering and providing all materials for this project. Many thanks are given for their commitment to providing tips and solutions for procedures. Thank you to their staff for helping me to frame the structure of this project. They were always available for answering questions and giving much guidance. Thank You!

REFERENCES

1. Calero-Cáceres, W., Ye, M., & Balcázar, J. L. Bacteriophages as environmental reservoirs of antibiotic resistance. *Trends in microbiology*. 2019.

2. Hillman, T. Current methods for inhibiting antibiotic-resistant bacteria by targeting bacterial cell metabolism and disrupting antibiotic elimination through the AcrAB-Tolc efflux pump. PeerJ Preprints 2019;7:e27840v1 https://doi.org/10.7287/peerj.preprints.27840v1

3. Lobanovska, M. and Pilla, G. Focus: Drug Development: Penicillin's Discovery and Antibiotic Resistance: Lessons for the Future? *The Yale journal of biology and medicine*, 2017; *90*(1), p.135.

4. Aminov, R. History of antimicrobial drug discovery: Major classes and health impact. *Biochemical pharmacology*, 2017;*133*, pp.4-19.

5. Landecker, H. Antibiotic resistance and the biology of history. *Body & Society*, 2016; *22*(4), pp.19-52.

6. Verstraeten, N., Knapen, W., Fauvart, M. and Michiels, J. A historical perspective on bacterial persistence. In *Bacterial Persistence* (pp. 3-13). Humana Press, New York, NY.2016

7. Eichenberger EM, Thaden JT. Epidemiology and Mechanisms of Resistance of Extensively Drug Resistant Gram-Negative Bacteria. Antibiotics. 2019 Jun;8(2):37.

1042 8. Rojo-Molinero, E., Macià, M. D., & Oliver, A. Social behavior of antibiotic-resistant mutants
1043 within Pseudomonas aeruginosa biofilm communities. *Frontiers in Microbiology*, 2019; *10*, 570.

1044 9. Singh, N., Romero, M., Travanut, A., Monteiro, P. F., Jordana-Lluch, E., Hardie, K. R., ... &
1045 Alexander, C. Dual bioresponsive antibiotic and quorum sensing inhibitor combination
1046 nanoparticles for treatment of Pseudomonas aeruginosa biofilms in vitro and ex vivo.
1047 *Biomaterials science*. 2019.

1048 10. France, M. T., Cornea, A., Kehlet-Delgado, H., & Forney, L. J. Spatial structure facilitates
1049 the accumulation and persistence of antibiotic-resistant mutants in biofilms. *Evolutionary*
1050 *Applications*, 2019; *12*(3), 498-507.

1051 11. Schiessl, K. T., Hu, F., Jo, J., Nazia, S. Z., Wang, B., Price-Whelan, A., ... & Dietrich, L. E.
1052 Phenazine production promotes antibiotic tolerance and metabolic heterogeneity in Pseudomonas
1053 aeruginosa biofilms. *Nature communications*, 2019;*10*(1), 762.

1054 12. Ardon, C. B., Prens, E. P., Fuursted, K., Ejaz, R. N., Shailes, J., Jenssen, H., & Jemec, G. B.
1055 E. Biofilm production and antibiotic susceptibility of Staphylococcus epidermidis strains from
1056 Hidradenitis Suppurativa lesions. *Journal of the European Academy of Dermatology and*
1057 *Venereology*, 2019;*33*(1), 170-177.

1058 13. Soares, A., Caron, F., & Etienne, M. Commentary: tolerance and resistance of pseudomonas
1059 aeruginosa biofilms to antimicrobial agents–how p. Aeruginosa can escape antibiotics. *Frontiers*
1060 *in Microbiology*, 2019; *10*, 2164.

1061 14. C.M. Waters, B.L. Bassler. Quorum sensing: cell-to-cell communication in bacteria. Annu.
1062 Rev. Cell Dev. Biol. 2005;21: 319-346.

1063 15. Zhang, X. X., & Rainey, P. B. Dual involvement of CbrAB and NtrBC in the regulation of
1064 histidine utilization in Pseudomonas fluorescens SBW25. *Genetics*, 2008; *178*(1), 185-195.

1065 16. Martínez JL, Rojo F. Metabolic regulation of antibiotic resistance. FEMS microbiology
1066 reviews. 2011 Sep 1;35(5):768-89.

1067 17. Sonnleitner, E., Valentini, M., Wenner, N., el Zahar Haichar, F., Haas, D., & Lapouge, K.
1068 Novel targets of the CbrAB/Crc carbon catabolite control system revealed by transcript
1069 abundance in Pseudomonas aeruginosa. *PloS one*, 2012; *7*(10), e44637.

1070 18. Shu YB, Peng B, Li H, Cheng ZX, Zhang TT, Zhu JX, Li D, Li MY, Ye JZ, Du CC, Zhang
1071 S. Pyruvate cycle increases aminoglycoside efficacy and provides respiratory energy in bacteria.
1072 Proceedings of the National Academy of Sciences. 2018 Feb 13;115(7): E1578-87.

1073 19. K. Ali, and T. Aruna. Recent advances in acetyl CoA carboxylase: a key enzyme of fatty acid
1074 biosynthesis in plants. Intl JAppl Biol Pharmac Technol. 2016;264-277.

1075 20. B.R. tenOever, The Evolution of Antiviral Defense Systems. Cell Host Microbe. 2016;
1076 19:142–149. doi: 10.1016/j.chom.2016.01.006.

1077 21. N. Nakashima, T. Tamura. Conditional gene silencing of multiple genes with anti-
1078 senseRNAs and generation of a mutator strain of Escherichia coli. Nucleic Acids Res. 2009;103
1079 (37).

1080 22. Francesc Vinals, Aachim Gross, Xavier Testar, Manuel Palacin, Peter Rosen, Antonio
1081 Zorzano, High glucose concentrations inhibit glucose phosphorylation, but not glucose transport,
1082 in human endothelial cells, Biochimica et Biophysica Acta (BBA) - Molecular Cell Research.
1083 1999; 1450(2)119-129, ISSN 0167-4889

1084 23. Siller, M., Janapatla, R.P., Pirzada, Z.A., Hassler, C., Zinkl, D. and Charpentier, E., 2008.
1085 Functional analysis of the group A streptococcal luxS/AI-2 system in metabolism, adaptation to
1086 stress, and interaction with host cells. BMC microbiology. 2008; 8(1), p.188.

1087 24. R.P. Ferraris, S. Yasharpour, K.C.K. Lloid, R. Mirzayan, J.M. Diamond, (1990) Luminal
1088 glucose concentration in the gut under normal conditions. Am. J. Physiol. 1990; 259, 820–837.

1089 25. M.M. Kendall, D.A. Rasko, V. Sperandio. Global effects of the cell-to-cell signaling
1090 molecule autoinducer-2, autoinducer-3, and epinephrine in a luxS mutant of enterohemorrhagic
1091 Escherichia coli." Infection and Immunity. 2007; 75(10):4875-4884.

1092 26. Labandeira-Rey, M., Janowicz, D.M., Blick, R.J., Fortney, K.R., Zwickl, B., Katz, B.P.,
1093 Spinola, S.M. and Hansen, E.J. Inactivation of the Haemophilus ducreyi luxS gene affects the
1094 virulence of this pathogen in human subjects. Journal of Infectious Diseases. 2009; 200(3):409-
1095 416.

1096 27. Osaki, T., Hanawa, T., Manzoku, T., Fukuda, M., Kawakami, H., Suzuki, H., Yamaguchi, H.,
1097 Yan,X., Taguchi, H., Kurata, S. and Kamiya, S. Mutation of luxS affects motility and infectivity
1098 of helicobacter pylori in gastric mucosa of a Mongolian gerbil model. Journal of medical
1099 microbiology. 2006; 55(11):1477-1485.

1100 28. U. Emilio. Shifts in metabolic hydrogen sinks in the methanogenesis-inhibited ruminal
1101 fermentation: a meta-analysis. Frontiers in Microbiology. 2015; 6(37).

1102 29. Jesudhasan, P.R., Cepeda, M.L., Widmer, K., Dowd, S.E., Soni, K.A., Hume, M.E., Zhu, J.
1103 and Pillai, S.D. Transcriptome analysis of genes controlled by luxS/autoinducer-2 in
1104 Salmonellaenterica serovar Typhimurium. Foodborne pathogens and disease.2010; 7(4):399-410.

1105 30. S.T. Freestone, B.L. Bassler. Bacterial Quorum Sensing: Its Role in Virulence and
1106 Possibilities for Its Control. Cold Spring Harbor Perspectives in Medicine. 2012; 2(11): a012427.
1107 doi:10.1101/cshperspect. a012427.

1108 31. J. Georg, R.H. Wolfgang. cis-antisense RNA, another level of gene regulation in bacteria.
1109 Microbiology and Molecular Biology Reviews. 2011; 75(2): 286-300.

1110 32. Vidal, J.E., Howery, K.E., Ludewick, H.P., Nava, P. and Klugman, K.P., 2013. Quorum-
1111 sensing systems LuxS/autoinducer 2 and Com regulate Streptococcus pneumoniae biofilms in a
1112 bioreactor with living cultures of human respiratory cells. Infection and immunity. 2013; 81(4):
1113 1341-1353.

1114 33. Trappetti, C., Potter, A.J., Paton, A.W., Oggioni, M.R. and Paton, J.C. LuxS mediatesiron-
1115 dependent biofilm formation, competence, and fratricide in Streptococcus pneumoniae. Infection
1116 and Immunity. 2011; 79(11):4550-4558.

1117 34. Peng B, Su YB, Li H, Han Y, Guo C, Tian YM, Peng XX. Exogenous alanine and/or glucose
1118 plus kanamycin kills antibiotic-resistant bacteria. Cell metabolism. 2015 Feb 3;21(2):249-62.

1119 35. Vendeville, A., Winzer, K., Heurlier, K., Tang, C.M. and Hardie, K.R., Making' sense of
1120 metabolism: autoinducer-2, LuxS, and pathogenic bacteria. Nature Reviews Microbiology. 2005;
1121 3(5):383.

1122 36. Li, J., Attila, C., Wang, L., Wood, T. K., Valdes, J. J., & Bentley, W. E. Quorum sensing in
1123 Escherichia coli is signaled by AI-2/LsrR: effects on small RNA and biofilm architecture.
1124 *Journal of bacteriology*, 2007; *189*(16), 6011-6020.

1125 37. Yang, Y., Zhou, M., Hou, H., Zhu, J., Yao, F., Zhang, X., Zhu, X., Hardwidge, P.R. and Zhu,
1126 G. Quorum-sensing gene luxS regulates flagella expression and Shiga-like toxin production in
1127 F18abEscherichia coli. Canadian Journal of microbiology. 2014; 60(6):355-361.

1128 38. A. Jayaraman, K.W. Thomas, Bacterial quorum sensing: signals, circuits, and implications
1129 for biofilms and disease. Annu. Rev. Biomed. Eng. 2008; 10:145-167.

1130 39. Vidal, J.E., Ludewick, H.P., Kunkel, R.M., Zahner, ¨ D. and Klugman, K.P. The
1131 LuxSdependent quorum-sensing system regulates early biofilm formation by Streptococcus
1132 pneumoniae strainD39. Infection and immunity. 2011; 79(10):4050-4060.

1133 40. E.S. James, J.E. Cronan. Expression of two *Escherichia coli acetyl-CoA* carboxylase subunits
1134 is autoregulated. Journal of Biological Chemistry. 2004; 279(4): 2520-2527.

1135 41. Tateda, K., Ishii, Y., Horikawa, M., Matsumoto, T., Miyairi, S., Pechere, J.C., Standiford,
1136 T.J., Ishiguro, M. and Yamaguchi, K. The Pseudomonas aeruginosa autoinducer N-3-
1137 oxododecanoylhomoserine lactone accelerates apoptosis in macrophages and neutrophils.
1138 Infection and immunity. 2003; 71(10), pp.5785-5793.

1139 42. Wozniak CE, Lin Z, Schmidt EW, Hughes KT, Liou TG. Thailandamide, a fatty acid
1140 synthesis antibiotic that is coexpressed with a resistant target gene. Antimicrobial agents and
1141 chemotherapy. 2018 Sep 1;62(9):e00463-18.
1142
1143 43. Long CP, Gonzalez JE, Cipolla RM, Antoniewicz MR. Metabolism of the fast-growing
1144 bacterium Vibrio natriegens elucidated by 13C metabolic flux analysis. Metabolic engineering.
1145 2017 Nov 1;44:191-7.
1146
1147 44. Berendonk TU, Manaia CM, Merlin C, Fatta-Kassinos D, Cytryn E, Walsh F, Bürgmann H,
1148 Sørum H, Norström M, Pons MN, Kreuzinger N. Tackling antibiotic resistance: the
1149 environmental framework. Nature Reviews Microbiology. 2015 May;13(5):310.

1150 45. Baquero F, Martínez JL. Interventions on metabolism: making antibiotic-susceptible bacteria.
1151 mBio. 2017 Dec 29;8(6):e01950-17.

1152 46. Wang, L., Hashimoto, Y., Tsao, C.Y., Valdes, J.J. and Bentley, W.E. Cyclic AMP (cAMP)
1153 and cAMP receptor protein influence both synthesis and uptake of extracellular autoinducer 2 in
1154 Escherichia coli. Journal of bacteriology. 2005; 187(6):2066-2076.

1155 47. Telford, G., Wheeler, D., Williams, P., Tomkins, P.T., Appleby, P., Sewell, H., Stewart,
1156 G.S., Bycroft, B.W. and Pritchard, D.I. The Pseudomonas aeruginosaquorum-sensing signal
1157 moleculen(3-oxododecanoyl)-l-homoserine lactone has immunomodulatory activity. Infection
1158 and immunity. 1998; 66(1):36-42.

1159 48. Wilson, J. W., Schurr, M. J., LeBlanc, C. L., Ramamurthy, R., Buchanan, K. L., and
1160 Nickerson, C. A. Mechanisms of bacterial pathogenicity. Postgraduate medical journal. 2002;
1161 78(918):216-224.

1162 49. Polyak SW, Abell AD, Wilce MC, Zhang L, Booker GW. Structure, function and selective
1163 inhibition of bacterial acetyl-CoA carboxylase. Applied microbiology and biotechnology. 2012
1164 Feb 1;93(3):983-92.

1165 50. Zuberi A, Misba L, Khan AU. CRISPR interference (CRISPRi) inhibition of luxS gene
1166 expression in E. coli: an approach to inhibit biofilm. Frontiers in cellular and infection
1167 microbiology. 2017 May 26;7:214.

1168 51. Hall CW, Mah TF. Molecular mechanisms of biofilm-based antibiotic resistance and
1169 tolerance in pathogenic bacteria. FEMS microbiology reviews. 2017 Mar 25;41(3):276-301.

1170

1171

1172

1173

1174

1175

1176

1177

1178

1179